Energetic Electron Interactions with Magnetic Islands in the Earth's Magnetosphere

by

Sydney Battles

A thesis submitted to the Graduate Faculty of
Auburn University
in partial fulfillment of the
requirements for the Degree of
Master of Science

Auburn, Alabama
August 8, 2026

Keywords: Magnetic islands, energetic electrons, MMS, geomagnetic storms

Approved by

Prof. Evdokiya Kostadinova, Chair, Assistant Professor, Physics Department
Prof. Hong Zhao, Associate Professor, Physics Department
Prof. Allen Landers, Professor, Physics Department

Abstract

This thesis investigates the interaction between magnetic islands and plasma electrons through analysis of data from NASA's Magnetospheric Multiscale (MMS) mission. To analyze MMS data, a semi-automated Python workflow was developed, which streamlines event selection based on bipolar signatures in the magnetic field and diagnostic plotting to detect magnetic islands. Data from the Fast Plasma Investigation (FPI) instrument and the Fly's Eye Energetic Particle Sensor (FEEPS) are used to analyze electron densities and energies for three distinct magnetic island structures – two in the magnetotail and one in the magnetosheath. In all cases, it was found that bulk plasma electron densities peak near island centers, or O-points, while bursts of energetic electrons were detected near island boundaries, or X-points. These findings mirror the behavior found in DIII-D magnetic islands, demonstrating that magnetic islands in magnetized plasma affect local electron densities and the observation of energetic electrons in both lab and space environments. Although the focus of this study is on observations of quasi-static islands, we also discuss how changes in magnetic island dynamics affect the resulting distribution of electron energies observed in both space and lab measurements. This study can further our understanding of cross-field transport processes relevant to both space weather prediction and fusion energy.

Artificial Intelligence (AI) Use Disclosure Statement

In the preparation of this thesis, no Artificial Intelligence (AI) tools were used.

Digital Accessibility Disclosure Statement

In the preparation of this thesis, the following digital accessibility tools were used to ensure this document complies with federal requirements: Microsoft Word Accessibility Checker. The author acknowledges full responsibility for the intellectual content of this work and has made a good faith effort to comply with digital accessibility requirements in publishing, wherein the nature of the content does not significantly change in order to do so. Furthermore, all content has been reviewed and revised to meet these requirements prior to final publication.

Acknowledgments

I would first like to express my deepest gratitude to my advisor, Dr. Kostadinova, for her guidance, patience, and support throughout my graduate studies. Her encouragement and thoughtful mentorship have been invaluable throughout the development of this thesis. I would also like to thank my thesis committee members, Dr. Zhao and Dr. Landers, for their time, insight, and thoughtful feedback throughout this process. I am grateful to the members of the Interdisciplinary Plasma Laboratory (IPL) for the discussions, encouragement, and support they provided throughout my time as a graduate student. I also acknowledge the support of National Science Foundation and U.S. Department of Energy, which made this research possible.

Finally, I would like to thank my family and friends, whose support carried me through the many challenges and milestones of graduate school. Thank you for reminding me who I am outside of my work, for celebrating the small victories, and for standing beside me through the difficult days. To my parents, thank you for instilling in me the belief that both curiosity and happiness are worth pursuing, even when the path is uncertain. This thesis carries the fingerprints of many people who encouraged me along the way, and I am deeply grateful for each of them.

Table of Contents

List of Figures

List of Abbreviations

MMS Magnetospheric Multiscale Mission

FPI Fast Plasma Investigation

FEEPS Fly's Eye Energetic Particle Sensor

FGM Fluxgate Magnetometer

Chapter 1 Introduction

Magnetized plasmas in both laboratory and space environments often form complex magnetic structures that strongly influence particle transport and energy conversion. For example, the formation of magnetic islands arises when magnetic reconnection or current-driven instabilities modify the configuration of magnetic field lines. These structures are commonly observed in laboratory fusion devices, such as tokamaks, as well as in natural space plasmas including the solar wind, heliospheric current sheet, and Earth's magnetosphere. Despite the differences in plasma parameters between these systems, magnetic islands consistently appear in regimes where magnetic energy is being converted into particle kinetic energy, making them a key structure for understanding plasma dynamics across scales.

In space plasmas, magnetic islands are frequently associated with reconnection-driven processes occurring in regions such as Earth's magnetotail. During solar wind–magnetosphere interactions, magnetic reconnection can form elongated current sheets that break up into multiple island-like structures. These structures are embedded within turbulent or semi-turbulent magnetic fields and are often linked to observation of increased particle acceleration and energy dissipation. Simulations of magnetotail reconnection have shown that electrons can be accelerated at localized regions such as island X-points and separatrices, where strong electric fields are present (Drake et al., 2006). Spacecraft observations over the past few decades have provided supporting evidence that energetic electron fluxes can increase near reconnection regions and within magnetic island chains, although interpretation is often limited by the single-spacecraft-trajectory nature of in-situ measurements.

In laboratory plasmas, magnetic islands play a similarly important role in determining transport and confinement properties. In tokamaks, islands can be produced by tearing modes or externally applied perturbations, leading to localized regions where magnetic flux surfaces are reconnected. These islands can significantly alter cross-field transport and can either degrade confinement or, in controlled settings, be used as a diagnostic or experimental tool for studying particle behavior. Experimental studies in devices such as DIII-D have shown that energetic electron populations can interact strongly with island structures, with evidence of both trapping and enhanced transport depending on the island configuration and background plasma conditions (Heidbrink and White, 2020; Joseph et al., 2008; Horton and Ichikawa, 1996).

A key feature shared between space and laboratory plasmas is that magnetic islands contain distinct topological regions that influence particle motion differently. The center of the island, often referred to as the O-point, corresponds to closed magnetic flux surfaces where particles can become trapped for extended periods. The X-points or separatrix regions represent locations where magnetic field lines reconnect and where strong gradients in the magnetic field and electric fields may accelerate or scatter particles. The competition between trapping in O-point regions and energization or scattering near X-points is therefore expected to play a central role in determining the energy distribution of electrons within magnetic islands and the presence of energetic electron populations.

An open question in both space and laboratory plasma physics is how energetic electron populations respond to these magnetic topologies across different regimes. While magnetic islands are known to form in both environments, it is not fully understood how electron acceleration, trapping, and transport scale with changes in magnetic field strength, plasma density, and system size. This includes questions such as whether energetic electrons tend to accumulate near X-points due to local acceleration mechanisms, or whether they become trapped within O-point regions depending on the island structure and evolution.

Recent experimental work in laboratory plasmas has further highlighted the role of magnetic topology in controlling electron transport. Studies motivated by DIII-D experiments have suggested that changes in island structure, including island bifurcation and stochastic magnetic field regions, can lead to significant changes in the distribution of suprathermal electrons (Eskew et al., 2026; Kostadinova et al., 2023). These results suggest that island geometry alone may be insufficient to fully explain electron transport, and that the interaction between islands and the surrounding magnetic structures must also be considered when interpreting particle behavior.

Spacecraft observations provide a complementary perspective. Missions such as NASA's Magnetospheric Multiscale (MMS) mission allow for high-resolution measurements of magnetic fields and particle distributions in regions where reconnection and magnetic island formation occur. These observations have confirmed that electron energization is often spatially localized and strongly correlated with magnetic structure, although interpreting detailed phase-space behavior remains challenging due to the rapid evolution of these systems and the limited spatial coverage of in-situ measurements.

The present study is motivated by these combined laboratory and space observations. It investigates how electron populations behave in the vicinity of magnetic islands observed in Earth's magnetosphere using MMS data. While laboratory results from tokamaks provide useful physical motivation, the primary focus of this work is on space plasma measurements and the characterization of electron behavior across different energy regimes within magnetic island structures. The goal is to identify whether consistent trends can be observed in the distribution of bulk and energetic electrons near island X-points and O-points, and to assess how these distributions relate to the underlying magnetic topology.

Finally, this work is motivated by the broader question of whether magnetic island topology represents a universal organizing structure for energetic electron dynamics across plasma environments. Although direct comparisons between laboratory and space systems require careful consideration of scaling and physical assumptions, identifying qualitative similarities in electron behavior may provide insight into the fundamental mechanisms governing particle transport in magnetized plasmas.

1.1 Magnetic Islands and Energetic Particles

Magnetic reconnection is a fundamental plasma process in which magnetic field lines change their configuration and release stored magnetic energy, causing particle acceleration, plasma heating, and bulk plasma motion. Magnetic fields govern the motion of charged particles throughout much of space and laboratory plasmas; thus, reconnection plays an important role in a wide range of environments including solar flares, planetary magnetospheres, astrophysical jets, and fusion devices (Yamada et al., 2010). Specifically, in Earth's magnetosphere, reconnection transfers energy from the solar wind into the near-Earth plasma environment and is one of the primary drivers of geomagnetic storms and substorms.

A simplified two-dimensional representation of magnetic reconnection is shown in Figure 1.1. Oppositely directed magnetic field lines are brought together within a thin current sheet where they reconnect and form new magnetic topologies. Plasma is accelerated away from the reconnection site while magnetic energy is converted into kinetic and thermal energy. Although reconnection is often represented using a two-dimensional geometry, the process is inherently three-dimensional and can generate a wide range of complex magnetic structures.

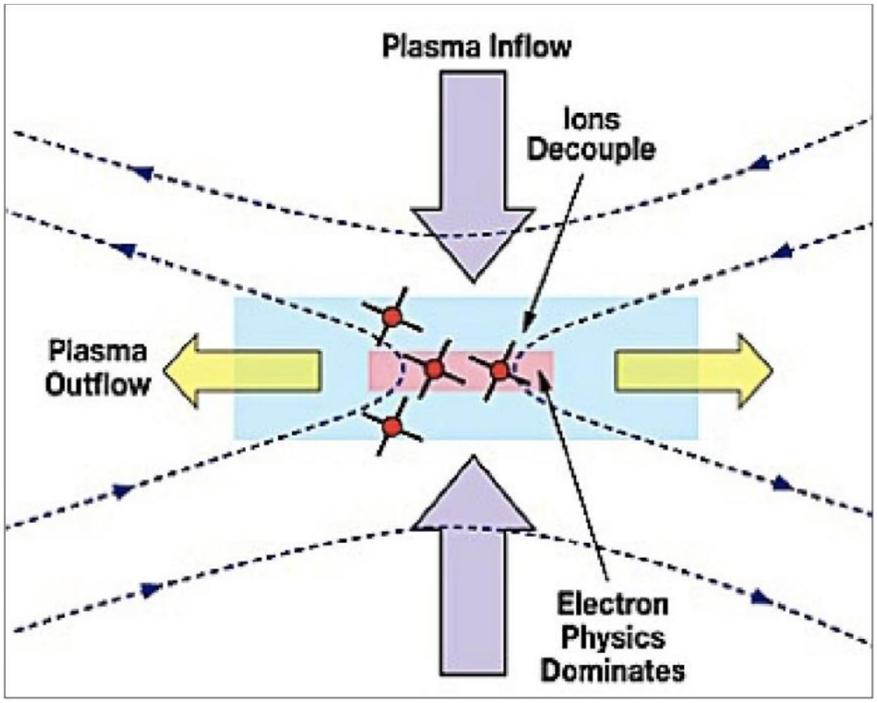

Figure 1. 1 Diagram of idealized magnetic reconnection geometry showing inflowing magnetic field lines, plasma outflows, and the reconnection X-point. (Image credit: NASA)

One of the most common consequences of magnetic reconnection is the formation of magnetic islands. Magnetic islands are localized magnetic structures consisting of closed or twisted magnetic field lines that become detached from the surrounding magnetic topology during reconnection. In three dimensions, these structures are often referred to as magnetic flux ropes, while the term magnetic island is commonly used when discussing two-dimensional cross sections through the structure or simplified reconnection geometries (Huang et al., 2019; Smith et al., 2024). Magnetic islands are characterized by distinct topological features, known as X-points and O-points. The island reconnection sites, where magnetic field lines break and reconnect, are known as X-points, while central regions of closed magnetic topology are known as O-points. An example magnetic island geometry is shown in Figure 1.2. The boundary surface separating magnetic field lines connected to the island from those connected to the surrounding plasma is known as the separatrix. Charged particles moving through these regions interact with substantially different magnetic topologies resulting in different transport behavior, which depends on their energy and pitch angle, where pitch angle is defined as the angle between a particle's velocity vector and the local magnetic field direction. Particles with different pitch angles follow different trajectories along and across magnetic field lines, influencing whether they become trapped within a magnetic island or escape into the surrounding plasma.

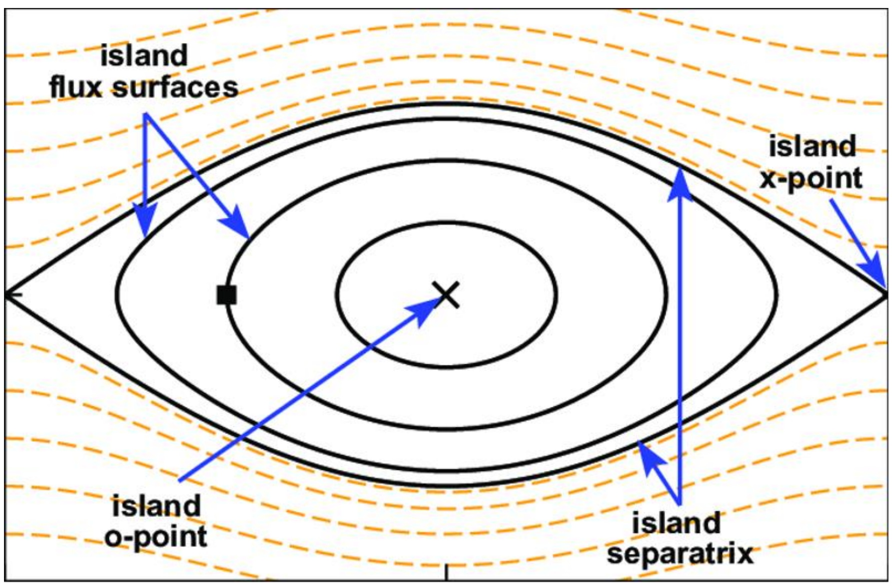

Figure 1. 2 Schematic magnetic island showing X-points, O-point, separatrix, and representative particle trajectories. (Image credit: Hölzl, 2010)

The distinction between X-point and O-point regions is particularly important when considering electron dynamics. Near the X-point, the magnetic field strength decreases substantially and particles may experience direct acceleration by reconnection electric fields. In contrast, the closed magnetic field geometry near the O-point can trap particles within the island interior for extended periods of time. This combination of acceleration near X-points and confinement near O-points makes magnetic islands natural laboratories for studying particle transport and energization processes in collisionless plasmas (Chen et al., 2008; Hasegawa et al., 2022).

The behavior of electrons within magnetic islands is often described in terms of bulk and energetic populations. Bulk electrons represent the majority of the plasma population and occupy energy ranges close to the thermal energy of the surrounding, or “background”, plasma. In magnetospheric plasmas, these energies are often on the order of tens of electron volts, depending on the plasma environment being considered. Energetic electrons, sometimes referred to as suprathermal electrons, occupy the high-energy tail of the distribution function and contain only a small fraction of the total particle population. Despite their relatively low abundance, energetic electrons often contain a significant fraction of the total plasma energy and can provide important information regarding the acceleration processes occurring within reconnection regions. Their larger velocities and gyro-radii allow them to interact with magnetic structures differently from lower-energy particles. As a result, energetic electrons frequently serve as tracers of acceleration mechanisms that may not be apparent when examining only bulk plasma moments.

The interaction of electrons with magnetic islands depends strongly on the relationship between particle gyro-radius and magnetic island size. Large ion-scale islands may trap both ions and electrons within their interiors, while smaller electron-scale islands primarily influence electron populations. This distinction between ion-scale and electron-scale structures has become increasingly important in recent years as improvements in spacecraft instrumentation have made electron-scale measurements possible (Torbert et al., 2018).

Several physical mechanisms have been proposed to explain particle acceleration in reconnection environments. One of the simplest mechanisms involves direct acceleration by the reconnection electric field near the X-point, where particles gain energy while crossing the diffusion region. This process is believed to contribute significantly to energetic particle production during magnetotail reconnection events and solar flares (Priest and Forbes, 2000). Additional acceleration mechanisms may occur after particles enter magnetic islands. One widely discussed mechanism involves Fermi acceleration within contracting islands, in which particles repeatedly reflect from converging magnetic structures and gain energy during each reflection. This process is similar to second-order Fermi acceleration originally proposed for cosmic rays and has been suggested as an efficient source of energetic electrons during reconnection events (Drake et al., 2006). Shock acceleration represents another possible source of energetic particles in space plasmas. In this mechanism, particles gain energy through repeated interactions with moving shock fronts. Although shocks are most commonly associated with planetary bow shocks and supernova remnants, turbulent reconnection environments may contain localized structures capable of producing similar acceleration (Yamada et al., 2010). In practice, multiple acceleration mechanisms may occur simultaneously within a reconnection region, making it difficult to identify the dominant process responsible for a given energetic particle population.

An active area of research is determining where energetic electrons are favorably located within magnetic islands, and how these electrons interact with the island. Early observations by Chen et al. (2008) reported enhanced energetic electron populations associated with magnetic island structures in Earth's magnetotail, providing some of the first observational evidence that magnetic topology strongly influences electron acceleration and transport. Since then, numerous studies have examined the relationship between energetic electrons and magnetic island topology. The launch of the Magnetospheric Multiscale (MMS) mission marked a significant advance in this effort by providing measurements with sufficient temporal resolution to resolve electron-scale structures directly. Using MMS observations, Torbert et al. (2018) reported the first direct measurements of the electron diffusion region during magnetic reconnection, demonstrating the ability of the mission to resolve electron-scale processes. Subsequent MMS observations have identified both ion-scale and electron-scale magnetic islands throughout Earth's magnetosphere. Huang et al. (2016) reported observations of ion-scale magnetic islands embedded within turbulent magnetosheath plasma and demonstrated the presence of energetic electron populations associated with these structures. Huang et al. (2019) later identified magnetotail flux ropes exhibiting strong energy dissipation and evidence of localized electron energization. More recently, Hasegawa et al. (2022) reported observations of an electron-scale magnetic island within an electron diffusion region, providing direct evidence that particle acceleration can occur even within extremely small magnetic structures. Large-scale surveys have also shown that magnetic islands and flux ropes are common features of the magnetotail environment rather than rare or isolated events. Smith et al.

(2024) performed an automated survey of MMS observations between 2017 and 2022 and identified large numbers of ion-scale magnetic flux ropes and loops throughout the magnetotail. These results suggest that magnetic islands may play a significant role in particle transport and energy conversion throughout Earth's magnetosphere, which in turn affects space weather events, such as geomagnetic storms.

Although considerable progress has been made in understanding particle acceleration during reconnection, a number of important questions remain unresolved. In particular, the relationship between magnetic topology and energetic particle transport is still not fully understood. The extent to which particle behavior depends on island size, magnetic geometry, and plasma environment remains an active area of research. Similarly, it remains unclear whether similar transport mechanisms operate across the broad range of plasma conditions encountered in laboratory and space environments. The present work contributes to this effort by examining electron populations associated with magnetic islands identified by MMS observations in both the magnetotail and magnetosheath. Attention is given to differences between lower-energy bulk electron populations and higher-energy electron populations near X-point and O-point regions in order to better understand the relationship between magnetic topology and electron transport.

1.2 Spacecraft Measurements in Earth's Magnetosphere

Many of the plasma processes responsible for particle acceleration occur naturally in Earth's magnetosphere, which is formed through the interaction of the solar wind with the terrestrial magnetic field. On the dayside, the magnetosphere is compressed by the incoming solar wind, while on the nightside it is stretched into a long magnetotail extending hundreds of Earth radii away from the planet. Magnetic reconnection occurs in both regions, although the magnetotail is more relevant to this study due to its large-scale current sheets and frequent reconnection events. The magnetotail current sheet also provides favorable conditions for the formation of quasi-static magnetic islands and flux ropes over a broad range of spatial scales. Because these structures evolve rapidly and often have sizes comparable to the gyro-radii of charged particles, in-situ spacecraft measurements are required to observe their dynamics and internal structure. Figure 1.3 shows a simplified diagram of Earth's magnetosphere, including the magnetotail and some of the major regions where reconnection is known to occur.

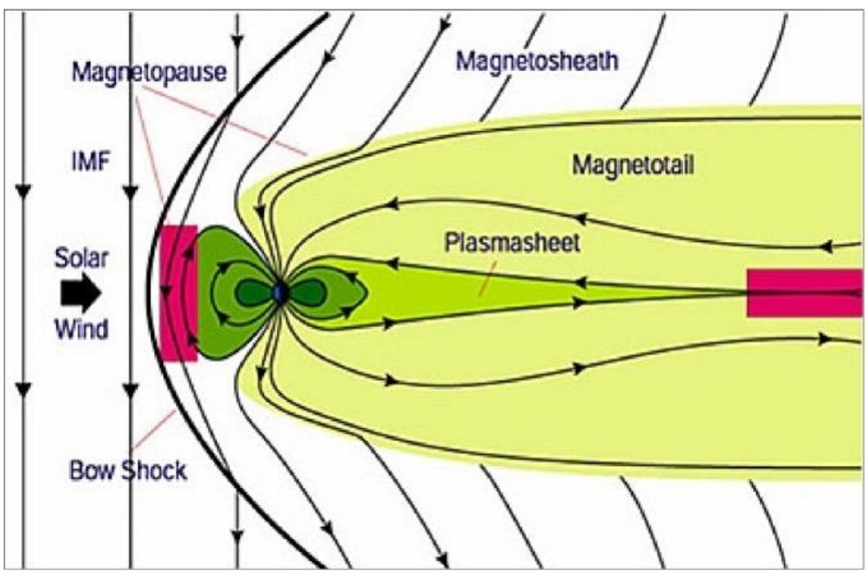

Figure 1. 3 Schematic of Earth's magnetosphere showing typical locations of magnetic reconnection and magnetic island formation, highlighted in red (Image credit: Southwest Research Institute)

Historically, the study of magnetic reconnection in space plasmas was limited by the capabilities of available spacecraft instrumentation. Earlier missions could measure large-scale magnetic field variations and plasma flows but lacked the temporal resolution needed to study electron-scale processes. Therefore, many fundamental questions regarding particle acceleration and energy conversion during reconnection remained unanswered.

One of the earliest missions designed specifically to study magnetospheric dynamics was the International Sun-Earth Explorer (ISEE) program during the late 1970s to early 1980s. Measurements from this mission provided some of the first direct observations of reconnection in Earth's magnetotail and established many of the observational signatures that continue to be used today, including magnetic field reversals associated with current sheet crossings (Paschmann et al., 1979).

Later missions expanded upon these observations. The Geotail mission, launched in 1992, explored the distant magnetotail and provided measurements of plasma flows and energy transport throughout the magnetosphere (Nishida, 1994). These observations contributed to the understanding of bulk flows, plasmoid formation, and magnetotail substorm dynamics. The Cluster mission, launched by the European Space Agency in 2000, offered a major advance in the study of magnetospheric plasmas. Cluster consisted of four identical spacecraft flying in formation around Earth. By observing the same plasma structures simultaneously from multiple locations, Cluster was able to distinguish between temporal variations and spatial structure in ways that had not previously been possible (Escoubet et al., 2001). Cluster observations provided important insights into magnetic reconnection in the magnetotail, including some of the earliest evidence that magnetic islands and flux ropes were common features of reconnection regions rather than isolated occurrences. These observations also contributed to early studies of energetic electron acceleration within reconnection environments and helped establish many of the physical questions that later motivated the MMS mission (Eastwood et al., 2010).

Unlike previous missions, MMS was designed from the beginning with electron-scale physics in mind. The spacecraft carry instruments capable of measuring three-dimensional electron distributions every 30 ms and ion distributions every 150 ms while simultaneously measuring magnetic and electric fields at extremely high cadence (Pollock et al., 2016; Russell et al., 2016).

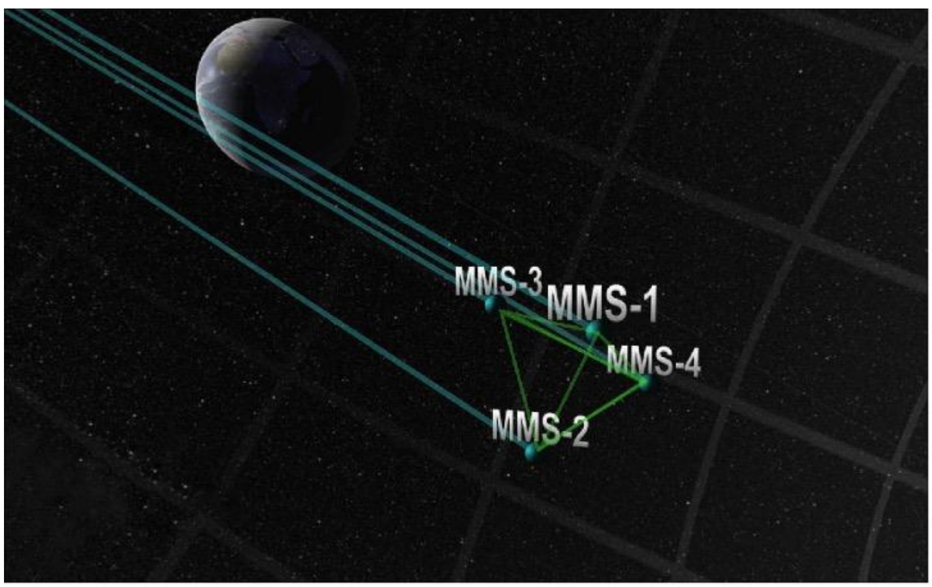

Figure 1. 4 Schematic of the MMS tetrahedral spacecraft configuration showing the relative positions of the four spacecraft during a typical observing campaign (Image credit: NASA)

The four-spacecraft configuration provides an additional advantage by allowing gradients and spatial derivatives to be estimated directly. This capability makes it possible to determine the orientation and motion of current sheets and magnetic structures while reducing uncertainties that often arise in single-spacecraft observations. A simplified illustration of the MMS tetrahedral configuration is shown in Figure 1.4. During different phases of the mission, spacecraft separations were adjusted to target ion-scale and electron-scale structures. Electron diffusion region studies required separations of only a few kilometers, comparable to characteristic electron kinetic scales within the magnetosphere.

The MMS orbit was designed to repeatedly sample regions where magnetic reconnection is expected to occur. During the first phase of the mission, the spacecraft focused primarily on dayside magnetopause reconnection. Later phases shifted the orbit toward the magnetotail, where the spacecraft encountered current sheets, flux ropes, and magnetic islands associated with substorm activity (Burch et al., 2016). The spacecraft velocity relative to magnetospheric structures varies significantly throughout the orbit and depends on both spacecraft motion and plasma velocities. Typical spacecraft velocities are sufficiently small compared to plasma flow speeds that magnetic islands and current sheets may often be approximated as stationary during individual crossings lasting only a few seconds. Under this assumption, temporal measurements obtained during a crossing can be interpreted as spatial cuts through the magnetic structure. This approximation provides an estimate of the characteristic size of magnetic islands observed by MMS. For example, a magnetic structure persisting for approximately two seconds during a crossing corresponds to a spatial scale on the order of several electron or ion inertial lengths, depending on the local plasma conditions and relative plasma flow velocity. The electron and ion inertial lengths are characteristic plasma scales that describe the distance over which electrons or ions begin to decouple from the collective motion of the plasma, making them useful reference scales for studying magnetic reconnection and other kinetic processes. Such estimates are frequently used in magnetospheric studies to classify structures as electron-scale or ion-scale islands (Torbert et al., 2018; Hasegawa et al., 2022).

The capabilities of MMS have enabled numerous studies of electron-scale magnetic reconnection and magnetic island dynamics that directly motivate the present work. Among the most relevant to this thesis, Hasegawa et al. (2022) reported observations of an electron-scale magnetic island embedded within an electron diffusion region, demonstrating that particle acceleration can occur even within extremely small magnetic structures. In addition, Smith et al. (2024) performed a statistical survey of MMS observations collected between 2017 and 2022 and showed that magnetic islands and flux ropes are common throughout Earth's magnetotail, indicating that these structures are a persistent feature of the magnetosphere rather than isolated events. Together, these studies demonstrate both the prevalence of magnetic islands and the importance of understanding how electron populations respond to their magnetic topology.

This work builds upon these previous observations by examining electron populations associated with several magnetic island events identified in both the magnetotail and magnetosheath. Rather than focusing exclusively on reconnection signatures themselves, the analysis emphasizes differences between lower-energy bulk electrons and higher-energy electron populations near X-point and O-point regions in order to better understand the relationship between magnetic topology and particle behavior.

1.3 Laboratory Studies of Magnetic Islands and Energetic Particles

Magnetic islands have also been extensively studied in magnetic confinement fusion devices. In tokamaks, magnetic islands form when perturbations in the magnetic field cause neighboring magnetic flux surfaces to reconnect and form closed helical structures. These islands can affect plasma transport, reduce confinement, and influence the behavior of energetic particles within the plasma. One of the primary concerns associated with magnetic islands in tokamaks is their interaction with energetic electrons. Under certain conditions, a population of highly energetic electrons, or runaway electrons, can form when the accelerating force from the electric field exceeds collisional drag within the plasma. Runaway electrons may reach relativistic energies, become de-confined from the plasma, and impact the wall of the fusion device, causing severe damage. Therefore, understanding how energetic electrons interact with magnetic topology is important for both plasma performance and machine protection in future fusion devices.

Magnetic islands can influence energetic electron transport in several ways. Depending on the magnetic geometry, energetic electrons may become trapped within the island interior, transported along island separatrices, or accumulate near regions of increased magnetic field curvature. The resulting particle distributions are often non-uniform and can evolve as the island grows, rotates, or interacts with surrounding plasma instabilities. The DIII-D tokamak has provided numerous opportunities to study these interactions experimentally. Operated by General Atomics in San Diego, California, DIII-D is a magnetic confinement fusion experiment that utilizes one of the most extensively diagnosed tokamaks currently in operation. Through a combination of magnetic diagnostics, soft X-ray measurements, and synchrotron emission imaging, DIII-D experiments have demonstrated that energetic electron behavior can exhibit strong correlations with magnetic island structures. For example, recent experiments at DIII-D utilized a fast camera with synchrotron emission filter, which showed that electrons with energies of ~10MeV are trapped within magnetic islands (Eskew et al., 2025). Because synchrotron radiation is produced when relativistic electrons are accelerated by magnetic fields, the measured emission provides a direct visualization of energetic electron populations. The concentration of synchrotron emission near island structures suggests that magnetic topology plays an important role in determining energetic electron transport and confinement.

Although the magnetic field strength, plasma density, and characteristic length scales differ substantially between tokamaks and Earth's magnetosphere, both systems contain magnetic islands generated through reconnection processes and both exhibit interactions between energetic particles and magnetic topology. This raises the possibility that some aspects of particle transport may be governed by physical mechanisms that are common across plasma environments despite large differences in global plasma parameters. Figure 1.5 compares a representative magnetic island observed in MMS measurements with a corresponding magnetic island reconstructed by a field line tracing code using inputs from DIII-D experiments. While the methods used to observe these structures differ significantly, both systems show evidence that energetic particles occupy preferred locations within the magnetic topology rather than being distributed uniformly throughout the plasma volume.

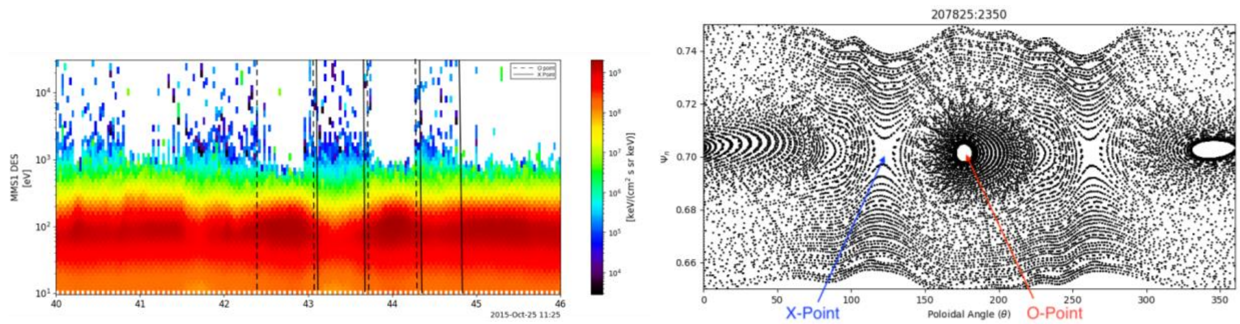

Figure 1. 5 Comparison between a magnetic island observed in Earth's magnetosphere (left) and a magnetic island observed in DIII-D (right). Despite large differences in scale and plasma conditions, both systems show non-uniform energetic electron distributions associated with magnetic toplogy.

In particular, this work examines whether energetic electrons in MMS observations typically occur near reconnection regions and island boundaries while lower-energy electron populations become concentrated within island interiors. Identifying such trends would provide a useful starting point for future studies aimed at understanding the extent to which particle transport processes may be shared across different plasma regimes.

1.4 Thesis Overview

The interaction between energetic electrons and magnetic topology remains an active area of research in both laboratory and space plasma physics. Although magnetic islands are observed in a wide range of plasma environments, many questions remain regarding how these structures influence particle transport, confinement, and acceleration. In particular, it is not yet clear to what extent electron dynamics observed in one plasma regime may be applicable to another.

Motivated by previous observations of energetic electron interactions with magnetic islands in both tokamak and magnetospheric plasmas, this work investigates the relationship between electron populations and magnetic island topology using observations from the Magnetospheric Multiscale mission. Focus is given to differences between lower-energy bulk electrons and higher-energy electron populations in the vicinity of magnetic island X-points and O-points.

The original motivation for this study arose from laboratory observations in the DIII-D tokamak, where energetic electrons have been observed to interact strongly with magnetic island structures. In some cases, magnetic islands may act as trapping regions that confine energetic electrons, while changes in island topology can lead to enhanced transport and the release of energetic particles from the plasma. Similar behavior has been reported in space plasmas, where magnetic islands generated during magnetic reconnection influence energetic electron distributions observed by MMS. These observations raise the possibility that magnetic topology may play a common role in energetic electron transport across widely different plasma environments. The primary hypothesis investigated in this work is therefore that the interaction of magnetic islands with different electronpopulations is characterized by qualitatively similar universal processes in both laboratory and space plasmas, despite large differences in magnetic field strength, density, temperature, and spatial scale. Specifically, this study explores whether energetic electron populations typically occur near reconnection sites and magnetic island boundaries while lower-energy bulk electron populations become concentrated within island interiors. We further conjecture that smaller and more dynamic islands lead preferentially accelerate bulk electrons through a reconnection process, while larger quasi-static islands efficiently accelerate already suprathermal electron populations to relativistic energies via a second-order Fermi process.

The analysis performed in this thesis focuses primarily on magnetic island observations in the Earth's magnetotail and magnetosheath using measurements from the MMS mission. Three previously identified magnetic island events are re-examined using a methodology designed to emphasize electron energy distributions over multiple energy ranges. Unlike many previous MMS studies that focus primarily on identifying reconnection signatures or determining magnetic topology, the present work places greater emphasis on the spatial distribution of electron populations within the underlying magnetic structures. Although qualitative comparisons are drawn between MMS observations and previously reported DIII-D measurements, the scope of the present study remains primarily focused on space plasma observations. Establishing a direct quantitative comparison between laboratory and magnetospheric magnetic islands would require additional analysis of plasma parameters, scaling relationships, and transport processes that extend beyond the scope of a Master's thesis. Nevertheless, identifying common trends in electron behavior may provide motivation for future studies aimed at understanding whether certain transport mechanisms are universal across plasma environments.

The remainder of this thesis is organized as follows. Chapter 2 introduces the Magnetospheric Multiscale mission and describes the spacecraft instrumentation, data products, and coordinate systems relevant to the present study. Chapter 3 describes the analysis methodology used to identify candidate magnetic island intervals and characterize electron populations using measurements from the FGM, FPI, and FEEPS instruments. Chapter 4 presents the results obtained from three MMS magnetic island events and compares electron behavior observed in different plasma environments and magnetic structures. Finally, Chapter 5 discusses the implications of these observations, the limitations of the current analysis, and possible directions for future work. While the present study represents only an initial investigation into energetic electron transport within magnetic islands, the results suggest that magnetic topology plays an important role in determining where energetic particles accumulate and how they evolve during reconnection events. Continued comparisons between laboratory and space plasma observations may therefore provide a useful approach for improving our understanding of energetic particle transport in magnetized plasmas.

Chapter 2 Magnetospheric Multiscale Mission

The Magnetospheric Multiscale Mission (MMS) is a mission developed by NASA to investigate the fundamental physics of magnetic reconnection in Earth's magnetosphere. As discussed in Chapter 1, magnetic reconnection plays an important role throughout plasma physics and astrophysics, including solar flares, planetary magnetospheres, laboratory plasmas, and fusion devices. Prior to MMS, many spacecraft missions had observed signatures of reconnection, but the spatial and temporal scales associated with electron dynamics remained difficult to resolve directly. The primary science objective of MMS is to investigate the electron diffusion region, the small region surrounding a reconnection site where electrons decouple from the magnetic field and conventional magnetohydrodynamic descriptions begin to break down. Resolving these scales requires measurements with substantially higher temporal resolution than those available from earlier space missions. To achieve this, MMS combines high-cadence plasma and field measurements with the ability to make simultaneous observations from four independent spacecraft.

Launched in March 2015, the mission consists of four identical spacecraft operated in a tetrahedral formation. By adjusting the separation distances between spacecraft, MMS can observe physical processes over a wide range of spatial scales, from ion scales down to electron scales. Spacecraft separations vary during different phases of the mission and have ranged from hundreds of kilometers to less than ten kilometers, allowing detailed investigation of kinetic plasma processes that were previously inaccessible to in-situ measurements. Figure 2.1 illustrates the tetrahedral spacecraft configuration used by MMS that allows simultaneous measurements at multiple locations within a plasma structure.

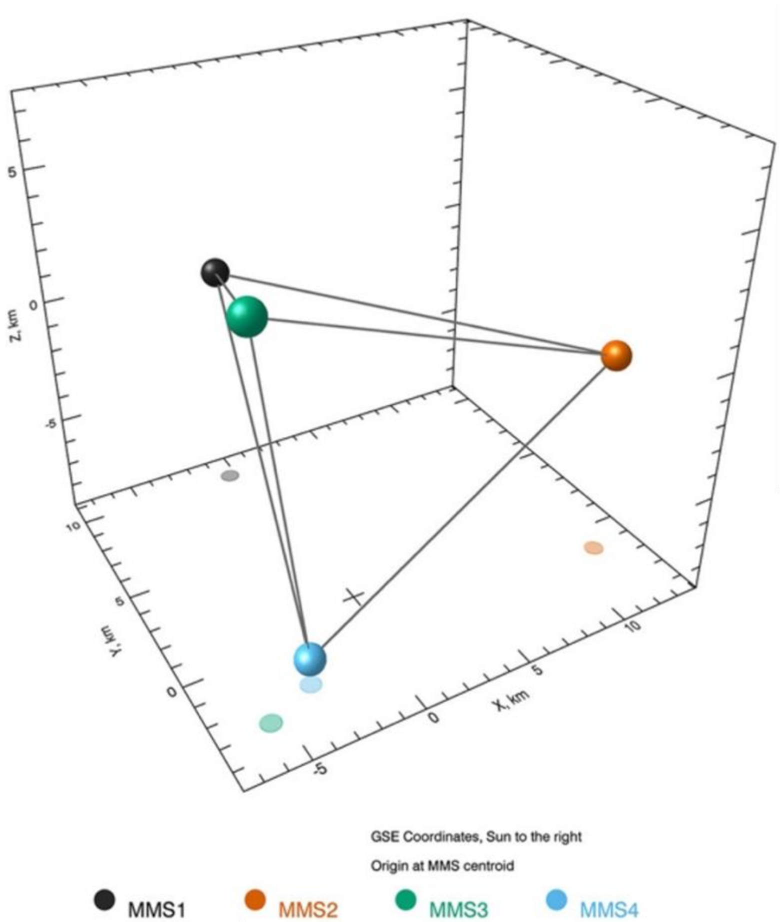

Figure 2. 1 Schematic of the MMS tetrahedral spacecraft configuration used to investigate 3D plasma structures (Image credit: NASA)

The MMS orbit was designed to sample multiple regions of Earth's magnetosphere where magnetic reconnection is expected to occur. The earlier phases of the mission primarily focused on the dayside magnetopause, where interaction between the solar wind and Earth's magnetic field drives reconnection. Later mission phases moved toward the magnetotail, allowing observations of reconnection occurring in the stretched current sheet on the nightside of the magnetosphere. Since magnetic islands and flux ropes frequently form in these regions, the magnetotail provides an ideal environment for studying electron behavior associated with reconnection.

The highly elliptical MMS orbit and the primary regions targeted during different mission phases are shown in Figure 2.2. Most of the events examined in this study occur in the magnetotail region, where MMS observations have provided some of the clearest evidence for electron-scale reconnection and magnetic island formation.

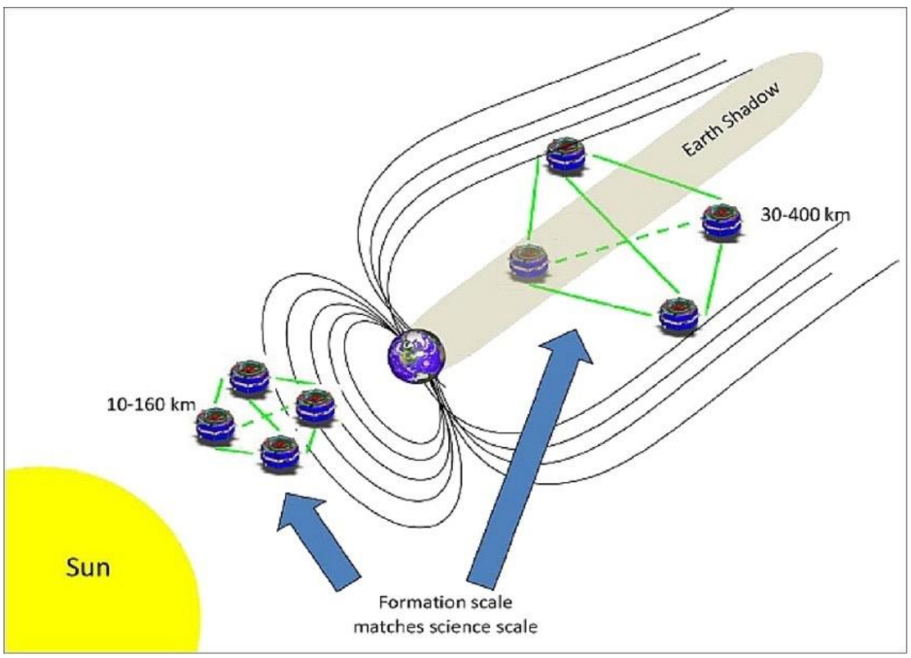

Figure 2. 2 Representative MMS orbit showing the dayside magnetopause and nightside magnetotail regions targeted during different phases of the mission (image credit: NASA)

The four-spacecraft configuration of MMS also enables the use of multi-spacecraft analysis techniques that can distinguish between temporal and spatial variations in the plasma environment. Although the present study utilizes measurements from a single spacecraft at a time, the availability of simultaneous observations from multiple spacecraft provides important context and has played a major role in the identification and characterization of many reconnection events reported in the literature.

An additional advantage of spacecraft observations is that temporal measurements can often be related to spatial structure. If a magnetic island evolves slowly compared to the time required for the spacecraft to cross it, the duration of the observed signatures can be used together with the spacecraft velocity to estimate characteristic spatial scales along the spacecraft trajectory. This approximation is commonly used when interpreting MMS observations of relatively stable magnetic structures and provides an important connection between time-series measurements and the underlying magnetic topology.

The combination of high temporal resolution measurements, multi-spacecraft observations, and adjustable spacecraft separations makes MMS uniquely suited for studying electron-scale magnetic reconnection and magnetic island dynamics. These capabilities have enabled numerous observations of electron diffusion regions, flux ropes, and magnetic islands throughout Earth's magnetosphere and form the foundation of this study. The analysis in this study uses measurements obtained from three instruments on the Magnetospheric Multiscale (MMS) spacecraft: the Fluxgate Magnetometer (Russel et al., 2016) , the Fast Plasma Investigation (Pollock et al., 2016), and the Fly's Eye Energetic Particle Sensor (Mauk et al., 2016). Together, these instruments provide detailed observations of the magnetic field and electron populations over a broad range of energies, allowing for the investigation of electron-scale magnetic islands. For each instrument, the following sections briefly describe the underlying measurement principles, the type of data products generated, and their relevance to the present analysis. Representative instrument schematics and example measurements are also included to provide context for the data products used in the analysis.

2.1 Coordinate Systems

Interpretation of spacecraft observations requires measurements to be expressed in a well-defined coordinate system. Because the orientation of the spacecraft changes continuously along its orbit and plasma structures may be aligned with the solar wind, Earth's magnetic field, or local current sheets, multiple coordinate systems are commonly used in magnetospheric physics. The choice of coordinate system often depends on the physical process under investigation and can significantly influence the interpretation of magnetic field and plasma measurements.

This study primarily uses the Geocentric Solar Ecliptic (GSE) coordinate system because it is the native coordinate system of many Level-2 MMS magnetic field products and provides a convenient framework for comparing measurements across events. In GSE coordinates, the origin is located at the center of the Earth, the positive X-axis points from the Earth toward the Sun, and the positive Z-axis points perpendicular to the ecliptic plane toward ecliptic north. The Y-axis completes the right-handed coordinate system and lies approximately in the dawn-dusk direction.

Within the magnetotail, these directions have useful physical interpretations. Variations in B_x are generally associated with changes in the tailward or Earthward magnetic field component, while variations in B_y correspond approximately to the dawn-dusk direction. The north-south magnetic field component B_z is of particular importance in reconnection studies because bipolar variations in this component are commonly associated with crossings of magnetic islands, flux ropes, and reconnection outflow regions. For this reason, the bipolar signature detection routine described in Chapter 3 focuses primarily on the temporal evolution of B_z.

Many studies of magnetotail reconnection instead use the Geocentric Solar Magnetospheric (GSM) coordinate system. Similar to GSE, the GSM coordinate system places its origin at the center of the Earth and defines the positive X-axis toward the Sun. However, the Z-axis is aligned with the projection of Earth's magnetic dipole axis onto the plane perpendicular to the Earth-Sun line, causing the coordinate system to rotate with changes in the dipole orientation throughout the year.

Figure 2.3 compares the orientations of the GSE and GSM coordinate systems.

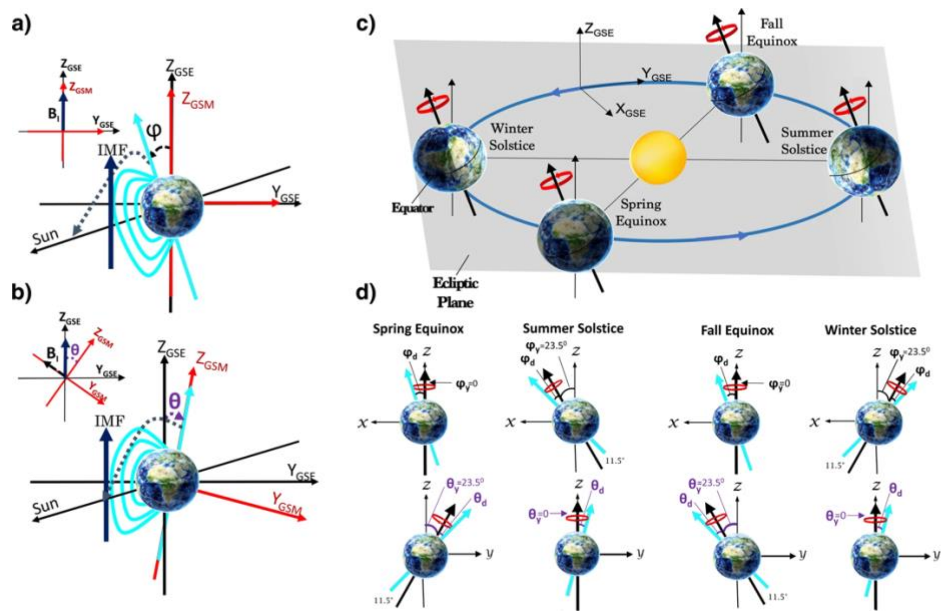

Figure 2. 3 (a) Earth's magnetic dipole (cyan) in GSM and GSE coordinate systems at the summer solstice, when dipole tilt φ is at its maximum of +35°. Black dashed lines show the angle between dipole axes and Sun-Earth line (b) Earth's magnetic dipole in GSM and GSE coordinates at the spring equinox (φ = 0°) (c) Earth's rotational axis (black), ecliptic plane (shaded gray), and GSE reference frame in context of Earth's orbit around the Sun (d) Earth's rotational axis (black) and Earth's magnetic axis (blue) throughout Earth's annual orbit. Top panel shows annual (φ_y) and daily (φ_d) variations of φ in X-Z GSM. Bottom panel shows annual (θ_y) and daily (θ_d) variations of θ (angle between GSE and GSM Z-axis). View is toward Earth from the Sun in Y-Z GSE plane. (Image credit: Kavosi et al., 2023)

Because GSM aligns more closely with the large-scale magnetic geometry of the magnetosphere, it is frequently used in studies of magnetotail current sheets and reconnection. Many of the magnetic island events discussed in the literature are therefore reported using GSM coordinates rather than GSE coordinates. Although this introduces small differences in the interpretation of individual field components, the overall signatures associated with magnetic islands remain largely unchanged.

In addition to global coordinate systems, studies of magnetic reconnection frequently employ a local coordinate system known as LMN coordinates. Unlike GSE and GSM, which are fixed relative to the Earth and Sun, the LMN coordinate system is constructed using the local magnetic field geometry of an individual reconnection event. The L-direction is chosen to lie along the reconnecting magnetic field component, the N-direction is defined as the normal direction to the current sheet, and the M-direction completes the right-handed coordinate system and is often associated with the out-of-plane current direction.

Transformation into LMN coordinates is commonly performed using techniques such as Minimum Variance Analysis (MVA), timing analysis using multiple spacecraft, or reconstruction methods based on local current sheet geometry. These approaches allow plasma flows and magnetic field variations to be interpreted relative to the reconnection region itself rather than to the Earth-Sun geometry. As a result, LMN coordinates are widely used in studies of electron diffusion regions and reconnection exhausts.

Although LMN coordinates provide a more physically intuitive description of reconnection geometry, this work primarily utilizes GSE coordinates for consistency with the publicly available Level-2 MMS products and to facilitate comparisons between multiple events. Because the primary objective of this work is the identification of magnetic island signatures and the examination of electron energy distributions rather than detailed reconstruction of current sheet geometry, GSE coordinates provide sufficient information for the analyses performed here.

2.2 Data Products and Operational Modes

The MMS Science Data Center distributes instrument measurements in several processing levels and operating modes designed to balance data volume with scientific requirements. Because this study focuses on electron-scale processes associated with magnetic reconnection and magnetic islands, only a subset of these products was used.

MMS data products are generally organized into Level-1, Level-2, and higher-level data sets. Level-1 products consist of minimally processed instrument measurements that have undergone basic formatting and decompression but have not yet been fully calibrated. Level-2 products contain calibrated and validated physical quantities derived from the raw instrument measurements and are intended for scientific analysis. Higher-level products, such as Level-3 and Level-4 data sets, include quantities derived from combinations of multiple instruments or spacecraft and often involve additional modeling or interpretation. All analyses performed in this study use Level-2 data products. This ensures that the magnetic field vectors, plasma moments, and particle energy measurements represent physically meaningful quantities that have been corrected for instrumental effects and transformed into standard coordinate systems where appropriate.

In addition to multiple processing levels, MMS instruments operate using several data acquisition modes with different temporal resolutions. The two primary modes are survey mode and burst mode. Survey mode provides continuous observations over long time intervals and is intended for identifying large-scale plasma structures and general magnetospheric conditions. Burst mode provides substantially higher temporal resolution measurements over shorter intervals, allowing rapidly evolving kinetic processes to be resolved. Because the characteristic timescales associated with electron-scale magnetic reconnection and magnetic island dynamics are extremely short, burst-mode data were used throughout this study. The higher measurement cadence available in burst mode allows the spacecraft to resolve the rapid magnetic field and plasma variations associated with these structures, whereas many of these features would be difficult or impossible to identify using survey-mode observations alone.

2.3 Fluxgate Magnetometer

Magnetic field measurements used in this work were obtained from the Fluxgate Magnetometer (FGM), which provides high-resolution vector measurements of the magnetic field. The instrument operates using the fluxgate principle, in which periodically driven ferromagnetic cores respond to external magnetic fields, allowing both the magnitude and direction of the field to be determined. Two triaxial sensor assemblies mounted on booms extending from the spacecraft minimize magnetic contamination arising from spacecraft systems. A photograph of one of the MMS fluxgate magnetometer sensors is shown in Figure 2.4.

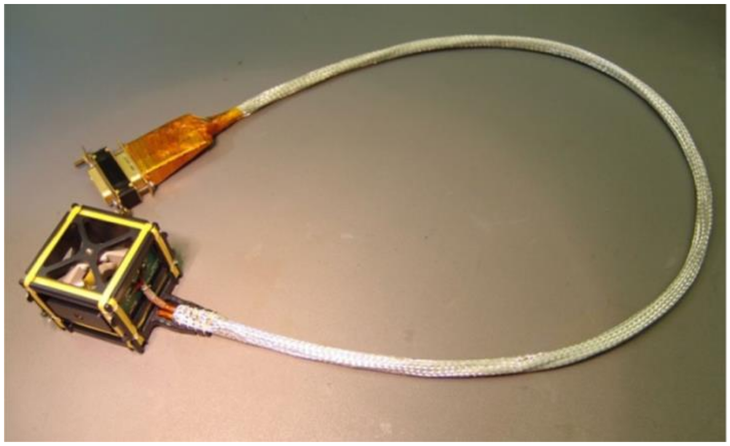

Figure 2. 4 Photograph of the MMS Fluxgate Magnetometer sensor (Image credit: MMS CMAD)

The physical measurement principle of a fluxgate magnetometer is based on electromagnetic induction and the magnetic response of ferromagnetic materials. An alternating current is passed through a drive coil surrounding a magnetic core, periodically driving the core into a fully magnetized state. In the absence of an external magnetic field, the magnetic response of the core is symmetric over each cycle. However, when an external magnetic field is present, this symmetry is broken, producing additional harmonic signals in a secondary sensing coil. The amplitude and phase of these induced signals are directly related to the strength and direction of the ambient magnetic field. The instrument electronics convert these induced voltages into calibrated magnetic field measurements along three orthogonal axes, producing the vector magnetic field components used in scientific analysis. The operating principle of a fluxgate magnetometer is illustrated schematically in Figure 2.5.

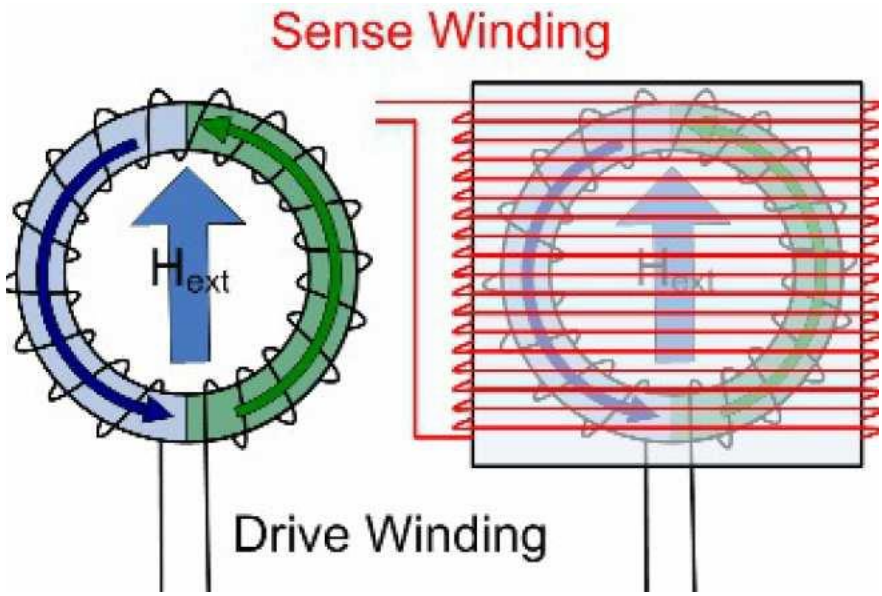

Figure 2. 5 General schematic of a single axis of fluxgate magnetometer sensor (Image credit: Imperial College London)

The raw output of the instrument therefore consists of time series measurements of the magnetic field along three independent directions defined by the spacecraft coordinate system. Following calibration and coordinate transformations performed by the MMS Science Data Center, these measurements are distributed as Level-2 data products in several standard coordinate systems, including Geocentric Solar Ecliptic (GSE) coordinates used in this work. The resulting data products consist of time-tagged magnetic field vectors, B_x, B_y, and B_z, typically reported in units of nanotesla (nT).

The FGM instrument provides continuous measurements of the magnetic field in several coordinate systems and at multiple temporal resolutions. In survey mode, magnetic field measurements are recorded at up to 16 vectors s^{-1}, while burst mode provides measurements at up to 128 vectors s^{-1}. In burst mode, the high sampling cadence enables the resolution of electron-scale magnetic structures associated with magnetic reconnection. In this study, Level-2 burst-mode magnetic field vectors in Geocentric Solar Ecliptic (GSE) coordinates were used to identify bipolar signatures indicative of magnetic island boundaries and other reconnection-related features.

2.3 Fast Plasma Investigation

Electron plasma measurements were obtained from the Fast Plasma Investigation (FPI) instrument, which was designed to characterize the three-dimensional velocity distributions of ions and electrons at a resolution sufficient enough to resolve electron-scale physics. The instrument consists of four Dual Electron Spectrometers (DES) and four Dual Ion Spectrometers (DIS), arranged to provide nearly full coverage.

The physical measurement principle of FPI is based on electrostatic energy analysis. Charged particles entering the instrument pass through a series of electrostatic deflection plates that selectively allow particles within a narrow range of energies and arrival directions to reach the detector. By continuously sweeping through different energy levels and combining measurements from multiple viewing directions, the instrument records the number of particles arriving with a given energy and velocity direction at a particular time. The raw output of the instrument therefore consists of particle counts as functions of energy and particle arrival direction. These directional measurements are combined to construct a three-dimensional velocity distribution function, which describes the number of particles moving with a given velocity in a particular direction. Following calibration and processing by the MMS Science Data Center, these distributions are converted into physically meaningful quantities such as phase space density and differential energy flux. The electron spectrometers measure the number of particles arriving from different directions and energies, thereby constructing a three-dimensional distribution function. From these distributions, plasma moments such as number density, bulk velocity, and temperature can be calculated through integration over velocity space. These moments provide information on plasma flows and density variations that are essential for identifying reconnection regions and describing magnetic island topology.

In addition to plasma moments, FPI provides energy spectra describing the distribution of electrons over an energy range extending from approximately tens of electronvolts to several tens of kiloelectronvolts. The analysis performed in this work primarily utilizes omni-directional electron spectra, which are obtained by integrating particle flux over all pitch angles. This approach produces energy distributions that are independent of the instantaneous magnetic field orientation and facilitates comparison between different magnetic structures and events. Because FPI produces complete three-dimensional distribution functions at high temporal resolution, it provides a detailed picture of electron behavior within reconnection regions, making it the primary diagnostic instrument used in the present study.

In the Earth's magnetosphere, typical plasma sheet electron populations are generally characterized by energies of several eV to tens of eV, while reconnection-associated acceleration processes can produce suprathermal and energetic electron populations extending into the keV range (Baumjohann and Treumann, 1996; Burch et al., 2016; Chen et al., 2011). During active reconnection events, localized electron acceleration near X-points and separatrices can produce enhanced high-energy populations that differ substantially from the surrounding background plasma (Chen et al., 2011; Wu et al., 2013). The FPI instrument measures the three-dimensional velocity distribution of thermal plasma particles, corresponding to the bulk electron population examined in this study. For burst-mode electron measurements, FPI covers energies from approximately 10 eV to 30 keV.

2.4 Fly's Eye Energetic Particle Sensor

Measurements of higher-energy electrons were obtained from the Fly's Eye Energetic Particle Sensor (FEEPS), which extends the observable energy range beyond that of the FPI instrument. FEEPS consists of multiple particle telescopes arranged to provide broad angular coverage and is specifically designed to measure energetic electrons and ions associated with particle acceleration processes.

The physical measurement principle of FEEPS differs from that of FPI. Rather than using electrostatic analyzers to select particles by energy, FEEPS directly detects energetic particles as they strike solid-state silicon detectors. When a charged particle enters one of the detector telescopes, it deposits energy within the detector material through interactions with the atomic electrons of the silicon. The magnitude of this deposited energy is proportional to the energy of the incident particle, allowing the instrument electronics to determine the particle energy. The raw output of the instrument therefore consists of particle counts recorded within discrete energy channels and viewing directions. Following calibration and processing by the MMS Science Data Center, these measurements are converted into differential particle intensities as functions of energy and time. The resulting data products provide information about energetic particle populations that are not accessible through standard plasma moment measurements. Compared with FPI, which primarily measures thermal and superthermal electrons, FEEPS is sensitive to particles in the tens to hundreds of kiloelectronvolt range. These energetic populations are of particular interest in studies of magnetic reconnection, where acceleration mechanisms can produce large deviations from the plasma thermal equilibrium.

This work uses omni-directional electron intensity measurements derived from the FEEPS telescopes. FEEPS measures suprathermal and energetic electrons over an energy range of approximately 30–600 keV, allowing higher-energy electron populations to be examined within the same magnetic structures observed by the FPI instrument. These measurements complement the lower-energy FPI observations by allowing analysis of energetic electron populations that may not be visible in standard plasma moment diagnostics. By combining information from FPI and FEEPS, electron distributions can be examined over multiple ranges in energy, allowing a more complete characterization of particle energization within magnetic island structures.

Chapter 3 Methodology

3.1 Data Sources and Computational Environment

The analysis presented in this work utilizes measurements obtained from the Magnetospheric Multiscale (MMS) mission. Data products were accessed through the MMS Science Data Center (SDC), which serves as the primary repository for mission data. This study focuses on electron-scale processes associated with magnetic islands and reconnection structures; therefore, high-time-resolution burst-mode observations were used throughout the analysis. Burst mode provides the highest temporal resolution available from the MMS instruments and, therefore, is well suited for analyzing the small spatial and temporal scales of electron dynamics in magnetic reconnection regions.

Measurements from three MMS instruments were used in this investigation. Magnetic field observations were obtained from the Fluxgate Magnetometer (FGM), which provides vector measurements of the magnetic field and enables the identification of bipolar magnetic signatures associated with magnetic islands (Russel, 2016). Electron plasma moments and energy spectra were obtained from the Fast Plasma Investigation (FPI) instrument, which measures three-dimensional particle distributions and provides quantities such as electron velocity and number density (Pollock, 2016). Higher-energy electron populations were examined using the Fly's Eye Energetic Particle Sensor (FEEPS), which extends the observable electron energy range of the FPI and allows investigation of energetic particle behavior within magnetic island structures (Mauk, 2016).

All data processing and analysis were performed using Python. Numerical calculations and array operations were carried out primarily using NumPy, while SciPy was used for signal processing and feature identification. Visualization and figure generation were performed using Matplotlib. Additional supporting libraries were used for data handling and interpolation where required.

The primary software framework used in this work was the Python Space Physics Environment Data Analysis Software, or PySPEDAS (Grimes et al. 2022). PySPEDAS is an open-source Python package developed for the retrieval, processing, and visualization of data from numerous space physics missions, including MMS. The package provides a unified interface for accessing mission data products and contains routines for data analysis. Its integration with the MMS Science Data Center enables automated downloading and loading of instrument data, providing a consistent framework for scientific analysis.

3.2 User Configuration and Data Retrieval

Prior to data processing, a set of user-defined parameters is specified to determine the MMS data to be analyzed. These parameters include the spacecraft number, the beginning and ending times of the time interval of interest, and the desired data acquisition rate. This structure provides a flexible framework that allows the analysis routine to be applied to multiple events without modification of the underlying code.

The user specifies one of the four MMS spacecraft together with a start and end time corresponding to the interval under investigation. The requested time interval is entered with a precision of one second, which defines the portion of the MMS dataset retrieved for analysis. Once loaded, the measurements retain their native instrument cadence, allowing plasma dynamics and magnetic island crossings to be resolved on much shorter timescales than the user specified interval. In addition, the data rate is selected according to the requirements of the analysis. Although both survey and burst modes are supported within the code, burst-mode data were used throughout this study because of the higher temporal resolution. Survey-mode data provide lower resolution measurements over extended periods of time and are useful for identifying large-scale plasma regions and candidate reconnection events. In contrast, burst-mode observations provide the temporal resolution necessary to examine electron-scale structures associated with magnetic reconnection. In this context, electron-scale structures refer to magnetic structures whose characteristic spatial and temporal scales are comparable to those of electron dynamics, as opposed to larger ion-scale structures that primarily influence ion behavior.

Once these input parameters are defined, the analysis routine automatically retrieves the corresponding Level-2 MMS data products through PySPEDAS. Data from the FGM, FPI, and FEEPS are downloaded and loaded into the Python environment for processing. This automated retrieval procedure eliminates the need for manual downloading and ensures that all data products corresponding to the selected interval are consistently obtained from the MMS Science Data Center. The configuration stage serves as the entry point for the analysis pipeline. After the desired spacecraft, time interval, and data products have been specified, the remainder of the algorithm proceeds automatically through a sequence of routines designed to identify candidate magnetic island signatures and examine the associated electron populations. The structure of the code allows for the analysis of multiple events while maintaining a consistent methodology across all intervals considered in this work.

3.3 Magnetic Field Analysis and Identification of Bipolar Signatures

Magnetic field measurements obtained from the Fluxgate Magnetometer (FGM) were used to identify candidate magnetic island crossings. Vector magnetic field data were extracted from the Level-2 burst-mode product and separated into their individual components in Geocentric Solar Ecliptic (GSE) coordinates. Particular attention was given to the B_z component of the magnetic field, since bipolar variations in this component are commonly associated with crossings of magnetic island boundaries and reconnection-related structures.

To identify candidate events, an automated bipolar signature detection routine was developed. The algorithm first locates zero crossings in the B_z component and then examines a finite interval surrounding each crossing. Within this search window, local maxima and minima are identified and used to determine the total magnetic field excursion. Candidate events are required to show a sufficiently strong bipolar variation relative to the local standard deviation of the magnetic field, therefore reducing the likelihood of false detections arising from background fluctuations or instrumental noise. To illustrate the comparison between a “strong” and “weak” bipolar signature, Figure 3.1

shows an example of magnetic field data from the FGM instrument. The yellow shaded region highlights an ideal bipolar B_z signature that exhibits a zero crossing and sufficient deviation from the localized magnetic field, as seen by the sharp dip-then-peak that ranges from approximately -60 nT to +30 nT. In contrast, a weak bipolar B_z signature highlighted in the blue region exhibits a zero crossing but lacks significant deviation, only spanning a range from -20 nT to +20 nT.

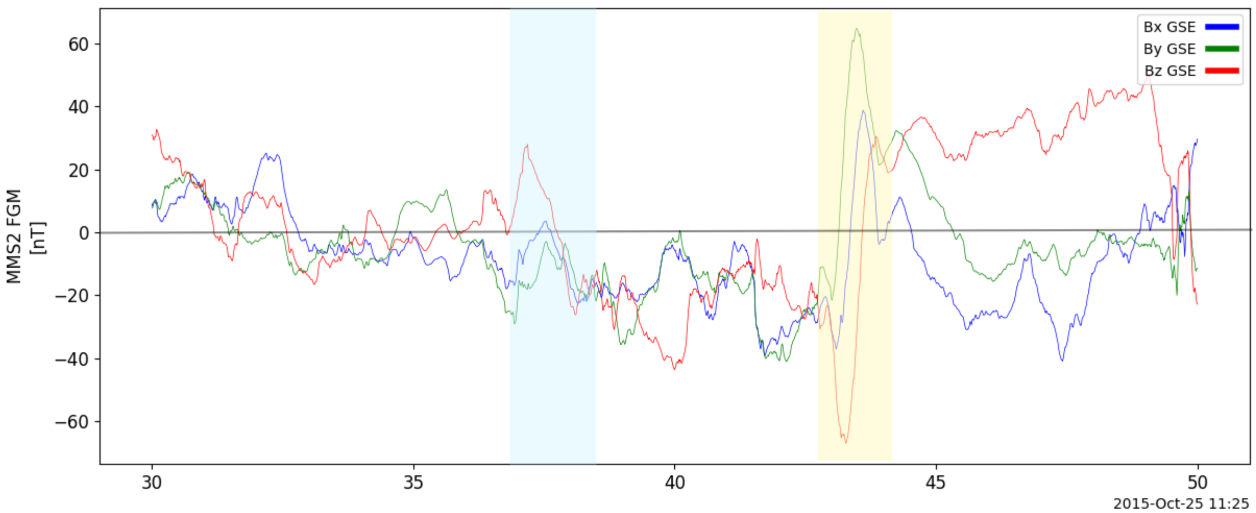

Figure 3. 1 Magnetic field component data from MMS2 spacecraft on October 25, 2015 displaying a bipolar signature in the GSE Z-direction at approximately 11:25:43 UTC, highlighted in yellow. The blue shaded region highlights an example of a bipolar signature in the Z-direction as well, but without significant enough deviation to warrant further analysis.

Additional constraints are imposed on the duration of the bipolar signatures. Events with durations shorter than one second or longer than four seconds are rejected, while neighboring detections separated by less than one second are merged into a single interval. The selected time window was based on the characteristic durations of bipolar signatures reported for magnetic island events in previous MMS studies, as well as the durations observed in the events examined in this work. The magnetic field reversals associated with the selected events typically occurred over approximately one to two seconds, while the four-second upper limit provided additional temporal padding to ensure that the full magnetic field structure surrounding the event was retained for analysis. These criteria were chosen to isolate localized magnetic structures while avoiding multiple identifications of the same event. A small temporal padding was applied to each interval to further ensure that the complete magnetic field variation associated with the structure was captured.

The start and end times of each detected bipolar signature were stored for use in subsequent stages of the analysis. These intervals provide reference times for examining electron moments and energy distributions associated with the candidate magnetic islands. In cases where no bipolar signatures were identified, the interval under consideration was excluded from further analysis.

Following event detection, the three magnetic field components were plotted as functions of time to provide a visual representation of the magnetic field evolution. These plots were used to verify the presence of bipolar structures and to place the identified intervals in the context of the surrounding magnetic field environment. Although the detection routine provides an automated means of identifying candidate events, visual inspection of the magnetic field profiles was used as an additional confirmation step to ensure that the selected intervals corresponded to physically meaningful structures. It is important to note that a bipolar magnetic field signature alone does not uniquely identify the underlying magnetic topology. Depending on the spacecraft trajectory and the local plasma environment, bipolar magnetic field signatures may be associated with crossings near reconnection X-points, magnetic island O-points, or other reconnection-related structures. Additional plasma measurements, including electron plasma moments and energy spectra, were therefore analyzed alongside the magnetic field observations to determine the most likely physical interpretation of each interval, following approaches used in previous MMS studies of magnetic islands (e.g., Huang et al., 2016). A schematic of a possible crossing geometry is provided in Figure 3.2 from Huang et al. (2019) observations of a flux rope in Earth's magnetotail.

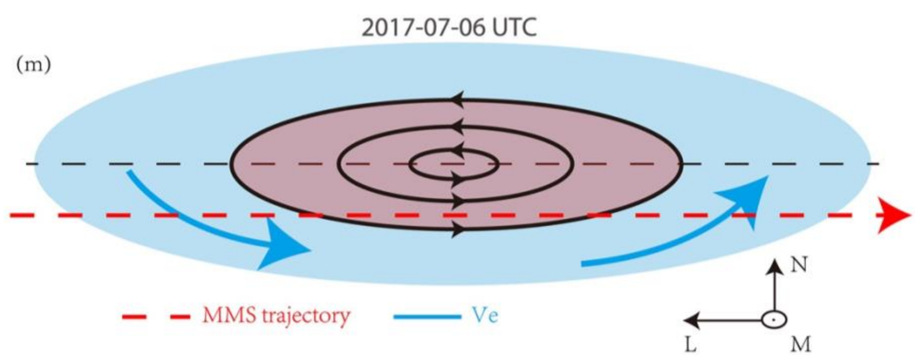

Figure 3. 2 Diagram of MMS trajectory across a magnetic island and corresponding electron flow in the LMN coordinate system. The cyan and red shadow indicate the exterior and interior regions of the island.

Although the bipolar detection algorithm was developed with the long-term goal of identifying candidate magnetic island events in larger MMS datasets, the events analyzed in the present study were selected from previously published observations in order to validate the analysis procedure against known magnetic structures.

3.4 Electron Plasma Moments: Velocity and Number Density

Electron plasma moments derived from the Fast Plasma Investigation (FPI) instrument were used to characterize the local electron populations detected during identified magnetic island intervals. In particular, the electron bulk velocity components and electron number density were examined to provide additional confirmation of magnetic island signatures and to aid in distinguishing between different regions of the observed structures. Variations in the electron velocity components were used to identify features such as flow reversals and stagnation regions, while changes in electron number density provided additional context for identifying regions associated with particle accumulation, such as magnetic island O-points.

The electron velocity distribution was obtained from the FPI moment product and visualized as time series of the three Cartesian velocity components. These measurements provide information on the bulk motion of the electron population and allow changes in the direction or magnitude of the electron flow to be identified. Such variations can provide evidence of plasma motion associated with magnetic reconnection and magnetic island structures when interpreted together with the magnetic field measurements. In addition, the electron number density was extracted from the corresponding FPI density moment product. The density evolution provides complementary information on electron trapping and rarefaction within and around magnetic islands. Variations in electron density are often associated with plasma pile-up regions near reconnection sites and can assist in distinguishing between different regions of the magnetic island topology.

3.5 Electron Energy Spectra (FPI and FEEPS)

Electron energy distributions were analyzed using data from both the Fast Plasma Investigation (FPI) and the Fly's Eye Energetic Particle Sensor (FEEPS) instruments in order to characterize particle populations across complementary energy ranges. Together, these instruments provide coverage from thermal and superthermal electrons through to higher-energy populations associated with reconnection and magnetic island dynamics.

3.5.1 FPI Electron Energy Spectra

Electron energy spectra in the approximate range $10^1 – 10^4$ eV were obtained from the FPI instrument using the omni-directional energy spectrogram product. The "omni" designation refers to the integration of electron flux over all pitch-angle directions, producing a scalar energy distribution that is independent of the magnetic field orientation. This representation is particularly useful in the present study, as the magnetic field topology evolves rapidly across reconnection regions and magnetic island boundaries, making fixed pitch-angle (parallel or perpendicular) distributions less suitable for consistent comparison across events.

Although pitch-angle resolved distributions (parallel and perpendicular to the local magnetic field) are available, the omni-directional spectra were selected in order to provide a robust and geometry-independent measure of electron energization. This allows direct comparison of energy distributions across different regions of the magnetic island without requiring continuous redefinition of the local magnetic field direction.

The FPI energy spectra were visualized using standard PySPEDAS time-series spectrogram routines. These spectrograms display the electron differential energy flux as a function of both time and energy, where color indicates the magnitude of the measured differential energy flux. The selected time intervals correspond directly to those identified through the magnetic field-based bipolar signature detection described in Section 3.3.

3.5.2 FEEPS Energetic Electron Spectra

Complementary measurements of higher-energy electrons were obtained using the Fly's Eye Energetic Particle Sensor (FEEPS), which extends the observable electron energy range beyond that of FPI into the tens to hundreds of keV regime. This instrument is essential for identifying energetic electron responses associated with reconnection outflows and magnetic island acceleration processes.

Unlike the FPI data products, the FEEPS energy spectra were not analyzed using the standard 'tplot' omni-directional spectrogram routine. Initial attempts to visualize the FEEPS distributions using analogous spectrogram formats did not yield clear signatures of localized enhancements, primarily due to the comparatively low particle counts at higher energies. As a result, energetic electron features are not readily visible in standard color-scale spectrogram representations, even when physically present. To address this limitation, a separate custom plotting routine was developed to analyze FEEPS energy distributions more directly. This routine was designed to examine integrated or binned energy counts over selected time intervals corresponding to identified magnetic island regions.

3.6 Energy Distribution Within Magnetic Island Regions

To investigate electron distributions within magnetic island structures, energy histograms were constructed for selected intervals corresponding to inferred X-point and O-point regions. Unlike the automated bipolar signature detection described in Section 3.3, the selection of these sub-intervals requires additional refinement based on combined visual and physical interpretation of the data. This step is therefore semi-automated and relies on the integration of multiple diagnostic quantities. Candidate X- and O-point regions were identified through a combination of (i) magnetic field structure, particularly bipolar signatures in B_z (ii) electron bulk velocity profiles, including stagnation or flow reversal regions, (iii) electron number density variations, and (iv) inspection of FPI electron energy spectrograms. X-point regions are typically associated with enhanced flow and reconnection outflows, whereas O-point regions are commonly characterized by electron accumulation and reduced flow speeds. These complementary signatures were used collectively to define time intervals for detailed energy analysis.

Once the intervals were selected, electron energy distributions were extracted from both the Fast Plasma Investigation (FPI) and Fly's Eye Energetic Particle Sensor (FEEPS) instruments. For each instrument, the particle intensity was averaged over the selected time window to obtain a histogram representing the energy distribution for the region of interest, with the vertical axis representing the time-averaged differential energy flux ($cm^{-2}\ sr^{-1}\ s^{-1}\ keV^{-1}$) and the horizontal axis representing the electron energies (eV-keV). Figure 3.2 shows example histograms from the two different instruments. Further analysis and physical interpretations of these plots are discussed in Chapter 4.

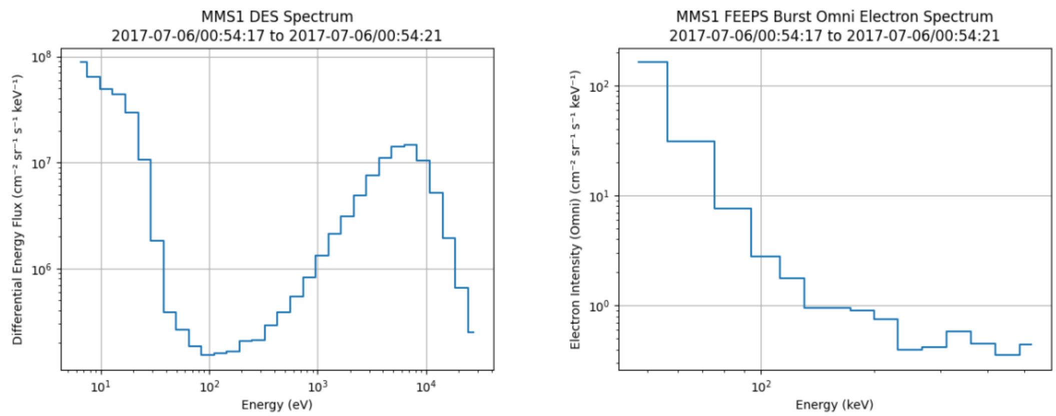

Figure 3. 3(a) Electron energy histogram (FPI) for the central region of the magnetic structure (O-point candidate interval). (b) Energetic electron histogram (FEEPS) for the central region of the magnetic structure.

In cases where FEEPS data were not available within the selected interval, the analysis was restricted to FPI measurements. This procedure allows for qualitative comparison of electron populations across multiple energy regimes within the same physical interval. In particular, it enables the identification of differences in the relative populations of low-energy and high-energy electrons between X-point and O-point regions, which may be indicative of localized acceleration processes associated with magnetic reconnection.

It is important to note that the selection of time intervals for this analysis is not fully automated and requires manual refinement based on the combined interpretation of magnetic field structure, plasma moments, and electron energy spectrograms. This approach ensures that the selected intervals correspond to physically meaningful regions within the magnetic island topology rather than purely algorithmic detections.

3.7 Summary of Analysis Workflow

The analysis procedure developed in this work consists of a sequential, multi-stage pipeline designed to identify magnetic island structures in MMS burst-mode observations and to characterize the associated electron dynamics across multiple energy regimes. The workflow integrates automated event detection with physically guided interval selection and multi-instrument plasma diagnostics.

The process begins with the specification of user-defined parameters, including spacecraft selection, time interval, and data rate. These inputs determine the set of MMS observations retrieved from the mission data archive through PySPEDAS. Magnetic field data from the Fluxgate Magnetometer (FGM), electron moments from the Fast Plasma Investigation (FPI), and energetic electron measurements from the Fly's Eye Energetic Particle Sensor (FEEPS) are then loaded and prepared for analysis. Following data retrieval, the magnetic field is analyzed to identify candidate magnetic island crossings. This is achieved through an automated detection algorithm applied primarily to the B_z component of the magnetic field, which isolates bipolar signatures indicative of magnetic topology changes. The resulting time intervals serve as preliminary event candidates and form the basis for further analysis.

Electron plasma moments, including bulk velocity and number density, are then examined within these intervals to provide contextual information on plasma flow structure and density variations. These quantities assist in distinguishing between different regions of the magnetic island, particularly in identifying stagnation regions associated with X-points and density enhancements characteristic of O-point regions.

Electron energy distributions are then analyzed using both FPI and FEEPS measurements. FPI provides energy spectra in the thermal to suprathermal range, while FEEPS extends coverage to higher-energy electrons. Energy spectra are initially examined over the full detected event interval and then refined through manual selection of sub-intervals corresponding to specific regions of interest within the magnetic island structure. To enable comparative analysis across instruments, electron energy distributions are further processed to construct normalized spectra on a common energy grid. This allows direct comparison of energy spectra between different spatial regions and energy regimes, allowing investigation of electron energization processes associated with magnetic reconnection. The final output of the workflow consists of a set of identified magnetic island events, each characterized by its magnetic field structure, electron flow properties, density variations, and energy distributions. This multi-stage approach ensures that event identification is both physically grounded and consistently applied across all analyzed intervals.

Chapter 4 Results

4.1 Overview of Selected Events

This chapter presents the results of the analysis applied to three selected magnetic island events observed by the MMS spacecraft. Two of the events are located in the magnetotail plasma sheet, while the third occurs in the magnetosheath. The magnetotail events are the focus of this study because the magnetotail current sheet is generally less turbulent than the magnetosheath environment, allowing magnetic structures to remain stable over longer time scales and making interpretation of particle behavior more straightforward. The magnetosheath event is included primarily as a point of comparison to investigate how electron behavior may differ in a more dynamic plasma environment. A more detailed discussion of the differences between magnetotail and magnetosheath plasma conditions is provided in Chapter 1. The events were chosen based on previously published studies identifying magnetic island or flux rope-like structures in these intervals and are re-examined here using a consistent analysis approach focused on electron-scale behavior.

The results are organized by event, with each section presenting the same sequence of diagnostic plots to allow for direct comparison between cases. These include magnetic field components from the Fluxgate Magnetometer (FGM), electron bulk velocity and number density derived from the Fast Plasma Investigation (FPI), and electron energy spectra from both FPI and the Energetic Particle Detector (FEEPS). In addition, selected time intervals within each event are further analyzed using energy histograms to examine how electron populations vary between different regions of the magnetic structure.

The primary goal of this analysis is to identify how electron populations respond to magnetic island-like structures across different plasma environments. In practice, this is done by combining magnetic field signatures with changes in electron velocity, density, and energy distributions, rather than relying on magnetic field data alone. Bipolar signatures in the magnetic field are used as a first indicator of candidate reconnection-related structures, which are then further examined using plasma moments and energy spectra to determine whether the surrounding electron population shows consistent signatures of electron trapping or energization. Each event is therefore assessed using the same set of observational criteria, but the interpretation focuses on how the electron response differs among events and plasma regimes. The following sections present the results for each event individually, beginning with the two magnetotail cases and concluding with the magnetosheath event, which provides a contrasting turbulent environment.

4.2 Magnetotail Event 1: July 06, 2017

The first event analyzed in this study occurs in the magnetotail on 6 July 2017 and is selected from previously reported observations of magnetic island-like structures in MMS burst-mode data (Norgren et al., 2020). In that work, multiple intervals from this day were identified as candidate magnetic islands based on characteristic magnetic field rotations and plasma signatures associated with reconnection in the magnetotail current sheet. The specific interval examined in this study (approximately 00:54:05–00:54:35 UTC) corresponds to one of these previously identified structures and is re-analyzed here with a focus on electron-scale behavior. While the original study primarily emphasized magnetic field topology and large-scale plasma structure, the present analysis focuses more on how electron velocity moments, density variations, and energy distributions evolve within the same interval. This event serves as a reference case for the magnetotail environment in this study. Previous MMS studies have shown that magnetic islands in the magnetotail often remain stable, or quasi-static, to allow investigation of particle dynamics within individual structures (Hasegawa et al., 2022; Smith et al., 2024). This event therefore provides a relatively clear example for examining electron-scale responses to localized magnetic topology and serves as a useful comparison point for the more dynamic magnetosheath event discussed later in this chapter.

4.2.1 Magnetic Field Signatures

The event was initially identified using the automated detection algorithm described in Chapter 3 and then verified through visual inspection of the magnetic field components. Figure 4.1 shows the magnetic field components B_x, B_y, and B_z (GSE coordinates), measured in nanotesla, as a function of time over the selected interval of 20 seconds.

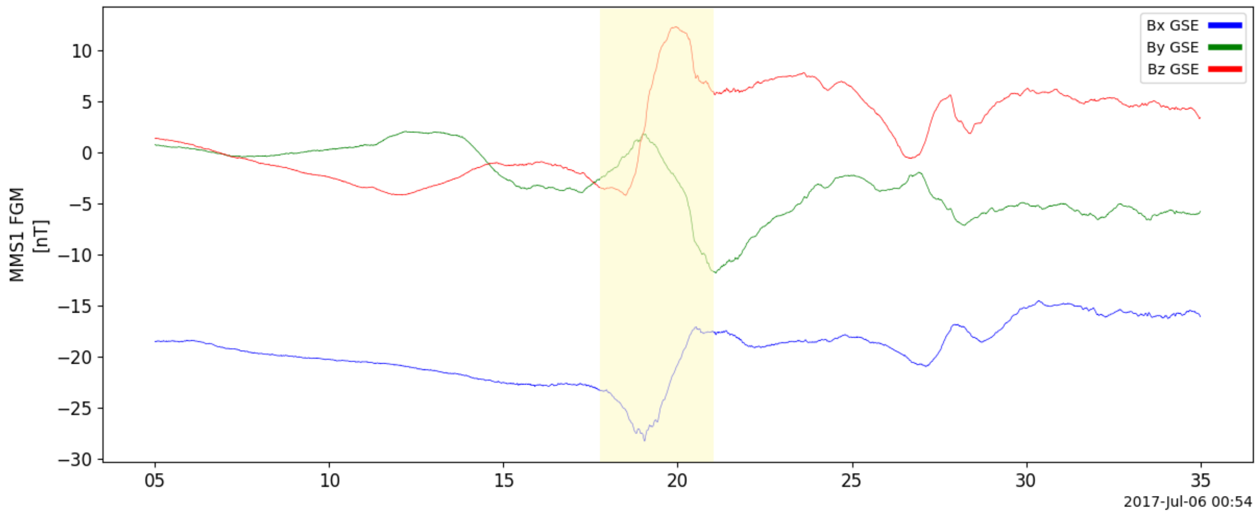

Figure 4. 1 Magnetic field components measured by the MMS FGM instrument in GSE coordinates during the selected magnetotail interval on 6 July 2017. The shaded region highlights the bipolar variation in B_z used to identify the candidate magnetic structure analyzed in this study.

As discussed in Chapter 2, the GSE coordinate system is oriented as follows: the x-direction points approximately toward the Sun, the z-direction is oriented normal to the ecliptic plane, and the y-direction completes the right-handed coordinate system. For magnetotail reconnection events, variations in the B_z component are of interest because localized reversals, or bipolar signatures, in this direction often indicate crossings of magnetic island structures.

A distinct bipolar variation is observed in the highlighted interval of the B_z component, characterized by a transition from positive to negative values over a timescale of approximately 1--2 seconds. This type of signature is consistent with a localized magnetic field reversal and is commonly associated with crossings of reconnection-related structures in the magnetotail. The duration of the observed bipolar signature is also consistent with the temporal scales expected for electron-scale magnetic structures discussed in Chapter 3.

It is important to note that the presence of a bipolar signature provides strong evidence for a localized magnetic structure, but it does not uniquely determine the topology of the event. As discussed in Chapter 2, such signatures may correspond to either reconnection X-point regions, magnetic island O-point crossings, or other boundary-related structures depending on the spacecraft trajectory. For this reason, additional plasma measurements are required to fully characterize the event.

4.2.2 Electron Velocity Signatures

To further investigate the nature of the structure, electron bulk velocity components, reported in GSE coordinates, from the Fast Plasma Investigation (FPI) instrument are shown in Figure 4.2 over the same time interval. The velocity data provides insight into plasma flow behavior in the vicinity of the detected magnetic structure.

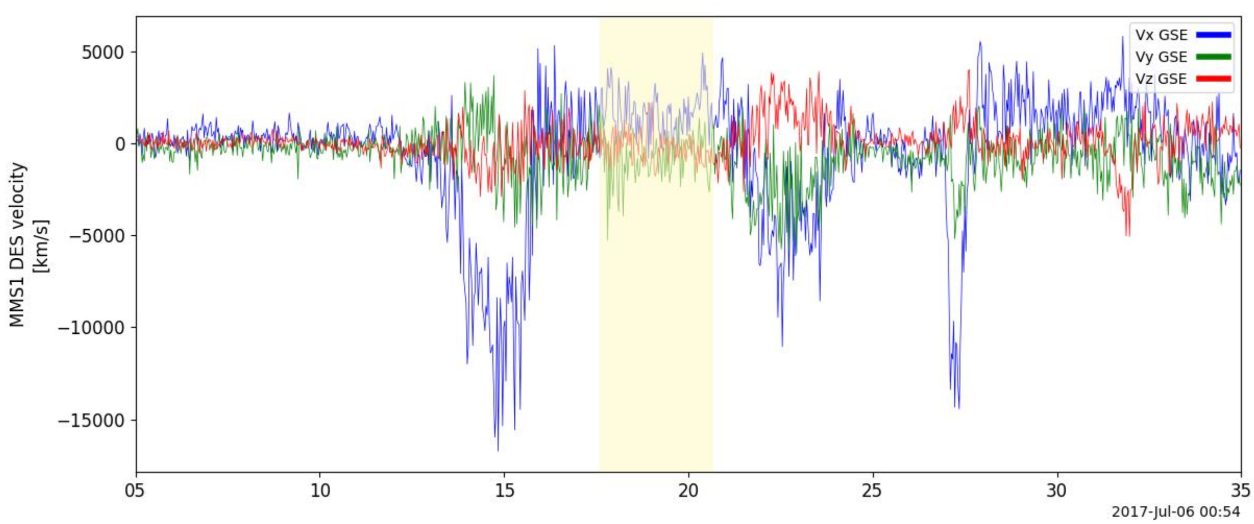

Figure 4. 2 Electron bulk velocity components in GSE coordinates for the selected magnetotail interval. The highlighted region corresponds to the bipolar magnetic signature shown in Figure 4.1 and indicates the interval used for comparison between magnetic and plasma measurements.

In magnetotail reconnection events, changes in the V_x component are often of interest because reconnection outflows frequently occur predominantly along the tail axis, producing enhanced Earthward or tailward plasma motion (Torbert et al., 2018). A notable feature of the event is the change in the electron velocity components within the highlighted interval, including a reduction in flow magnitude near the center of the bipolar magnetic signature. This behavior is consistent with the presence of a stagnation region, where plasma flow slows or changes direction due to the local magnetic topology. Such regions are commonly associated with transitions between inflow and outflow regions in reconnection geometries.

The largest velocity variations are observed in the V_x component, where the electron bulk flow changes substantially on either side of the stagnation region. This behavior is consistent with reconnection-driven plasma motion in the magnetotail and suggests that the spacecraft is crossing a region of plasma flow rather than a uniform background environment. Combined with the bipolar magnetic field signature, these velocity variations suggest that the spacecraft crossed a magnetic structure, such as a magnetic island, associated with reconnection activity.

4.2.3 Electron Number Density

Figure 4.3 presents the electron number density over the same interval. The density profile exhibits a localized variation comparable with the magnetic field and velocity signatures identified in the previous sections.

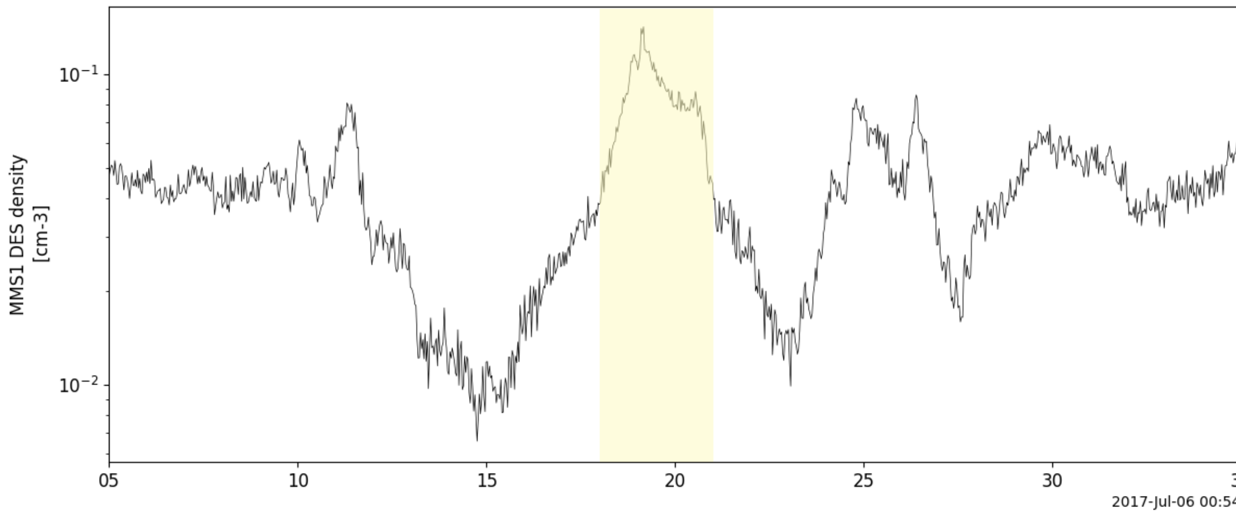

Figure 4. 3 Electron number density measured by the MMS FPI instrument during the selected magnetotail interval on 6 July 2017. The highlighted region corresponds to the bipolar magnetic field signature identified in Figure 4.1. The observed density enhancement near the center of the event is examined as a possible indicator of electron accumulation within the magnetic structure.

An enhancement in electron density is observed near the central portion of the event. This behavior is consistent with particle accumulation in confined magnetic structures, such as the central region (O-point) of a magnetic island. However, the magnitude and sharpness of this enhancement vary depending on the exact location within the structure and the spacecraft trajectory. The combined observation of density variation and velocity stagnation provides additional support in the identification of a potential magnetic island.

4.2.4 FPI Electron Energy Spectra (Bulk Population)

The electron energy spectrum measured by the Fast Plasma Investigation (FPI) instrument is shown in Figure 4.4 for the duration of the event. The FPI energy range primarily covers the thermal and suprathermal electron population, typically spanning energies from approximately 10^1 to 10^4 eV.

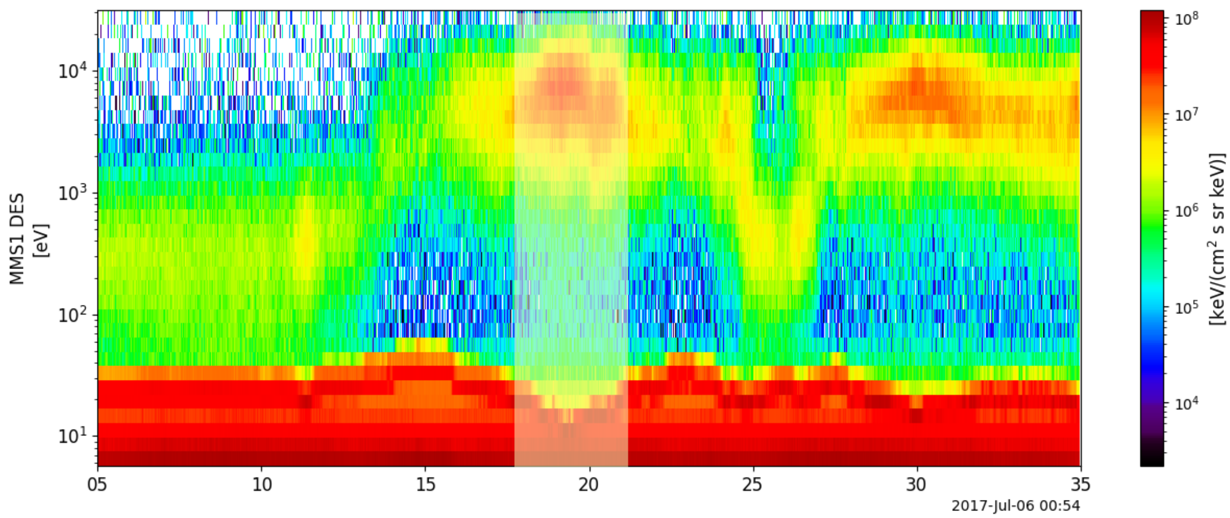

Figure 4. 4 Omni-directional electron energy spectrum measured by the MMS FPI instrument during the selected magnetotail interval on 6 July 2017. The shaded region corresponds to the bipolar magnetic field signature identified in Figure 4.1. The spectrogram reveals a low-energy bulk electron population near 10 eV together with a localized enhancement of electrons near 10^4 eV within the magnetic structure.

The spectrum is presented as an omni-directional distribution, representing an integration over all directions and pitch angles. This provides a measure of the total electron intensity as a function of energy that is independent of the magnetic field orientation, allowing changes in the overall electron population to be identified more clearly. The color scale represents the omni-directional differential energy flux measured by the instrument, with larger values corresponding to greater populations of electrons at a given energy and time.

Several distinct electron populations can be identified within the spectrogram. Throughout much of the interval, a high-density bulk electron population is observed near energies of approximately 10 eV, corresponding to the thermal background plasma, as seen from the red color band on the bottom of Fig. 4.4. A second, less intense population is present at intermediate energies between approximately 10^2 and 10^3 eV outside of the magnetic structure, as seen from the green color region visible between approximately 5-12s on Fig. 4.4. However, within the highlighted interval corresponding to the bipolar magnetic signature identified in Fig. 4.1, a pronounced enhancement in electron intensity appears near energies of approximately 10^4 eV near the center of the structure, as highlighted by the pink rectangle in Fig. 4.4. At the same time, the intermediate-energy population in this region becomes reduced within the structure, producing a clearer separation between the low-energy bulk electrons and the higher-energy suprathermal electrons. The appearance of this concentrated population of energetic electrons near the center of the event is consistent with the interpretation that electron energization and trapping processes are occurring within the magnetic structure. Together with the magnetic field, velocity, and density measurements presented previously, the energy spectrum provides additional evidence that the spacecraft crossed a magnetic island-like structure in the magnetotail.

4.2.5 FEEPS Higher-Energy Electron Measurements

Although the FEEPS instrument measures electrons at substantially higher energies than the FPI instrument, the electron population within this energy range is much smaller. As a result, the omni-directional energy spectrogram shown in Figure 4.5 does not exhibit the same clearly defined structures observed in the FPI spectrogram. While a slight enhancement in electron intensity is visible near the time of the magnetic island crossing, the low count statistics make it difficult to identify localized features directly from the spectrogram. For this reason, the FEEPS measurements are analyzed using time-averaged energy distributions rather than spectrograms. Averaging over selected intervals improves the counting statistics and provides a clearer representation of the energetic electron population associated with the magnetic structure.

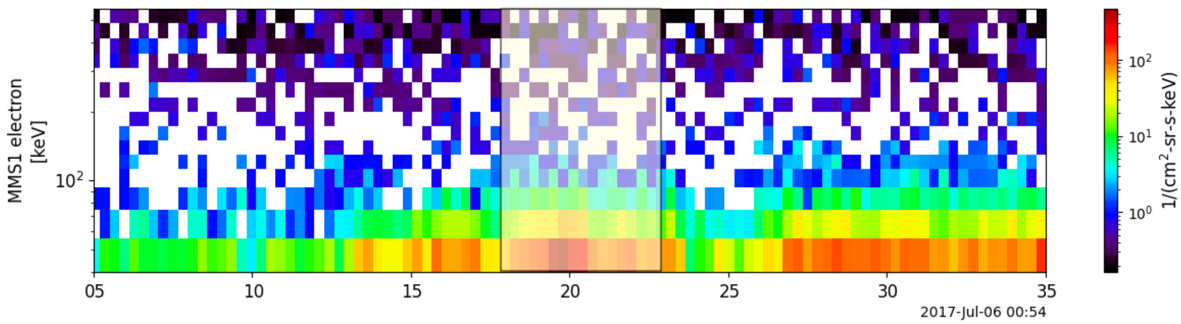

Figure 4. 5 Omni-directional electron energy spectrogram measured by the FEEPS instrument during the selected interval. The highlighted region corresponds to the magnetic structure identified in Figure 4.1. Due to the relatively low energetic electron density, localized features are not clearly resolved in spectrogram form, motivating the use of time-averaged energy distributions in the following section.

4.2.6 Electron Energy Distributions

The electron energy distributions derived from both the FPI and FEEPS instruments are shown in Figure 4.6. The distributions correspond to the interval associated with the expected O-point identified from the combined magnetic field, velocity, and density analysis presented in the previous sections. Examining the two instruments together provides a more comprehensive view of the electron population from approximately 10 eV to hundreds of keV.

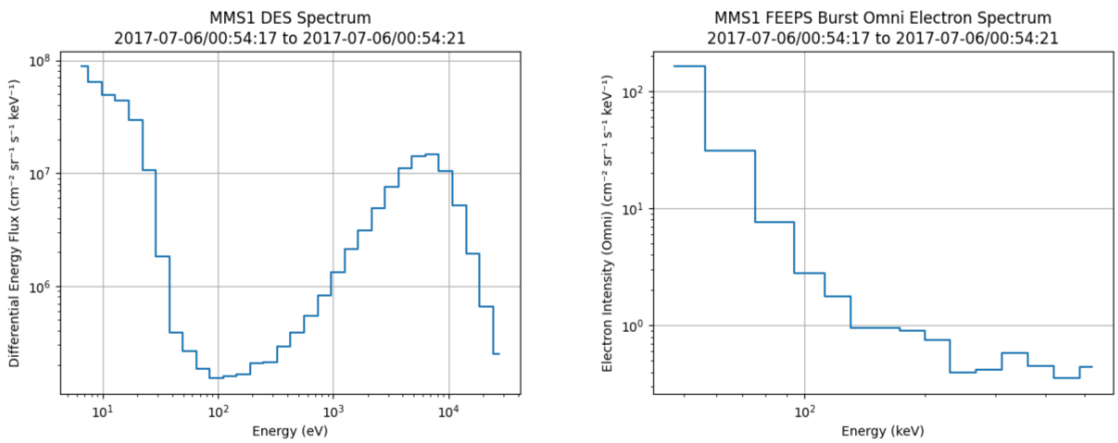

Figure 4. 6 (a) Electron energy distribution derived from the FPI instrument for the interval corresponding to the expected O-point. Two distinct electron populations are observed: a dominant bulk population near 10 eV and a broader suprathermal population extending from approximately 1 keV to 10 keV. A reduced electron population is present near approximately 100 eV. (b) Electron energy distribution derived from the FEEPS instrument for the same interval shown in Figure 4.6(a). The distribution extends the observable energy range into the tens to hundreds of keV, displaying the presence of a smaller population of energetic electrons beyond the energy range measured by FPI.

The FPI energy distribution (Figure 4.6a) reveals two distinct electron populations. The dominant population is centered near approximately 10 eV and represents the background bulk electron population. A second population is observed between approximately 1 keV and 10 keV, with a broad peak near 5–6 keV. Between these populations, the electron distribution decreases substantially near approximately 100 eV, producing a noticeable reduction in the intermediate-energy range.

The FEEPS energy distribution (Figure 4.6b) extends the observable energy range into the tens to hundreds of keV. Although the energetic electron population is much smaller than the bulk population observed by FPI, electrons are detected at energies approaching 10^2 keV (100 keV), demonstrating that a small population of highly energetic electrons is present within the interval.

Finally, Figure 4.7 shows a reference interval prior to the structure crossing using FPI data. In this pre-event region, the electron energy distribution exhibits a more continuous spectrum extending through the intermediate-energy range (approximately 100 eV), which becomes significantly reduced once the spacecraft enters the magnetic structure. This suggests a reorganization of the electron population associated with the transition into the magnetic island-like region.

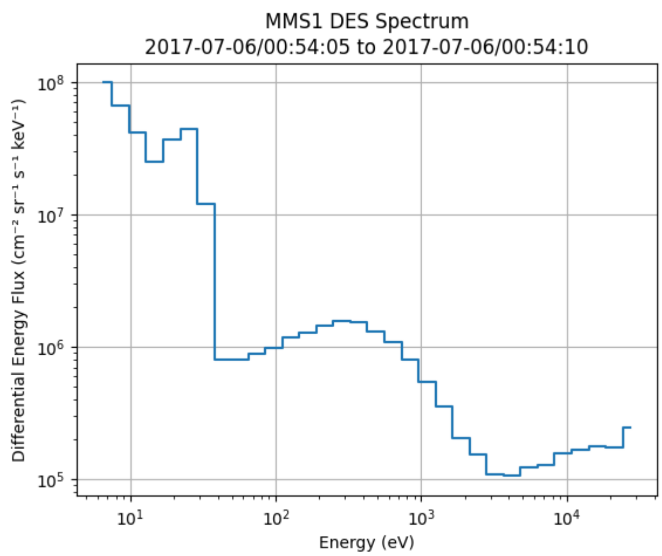

Figure 4. 7 Electron energy histogram (FPI) for a pre-event reference interval prior to the magnetic structure crossing. The distribution shows a more continuous spectrum extending through the intermediate-energy range (~100 eV), which becomes reduced during the magnetic structure encounter.

Together, the FPI and FEEPS measurements demonstrate that the electron population spans several orders of magnitude in energy, ranging from the background bulk plasma near 10 eV to energetic electrons approaching hundreds of keV. The implications of these distinct electron populations and their relationship to magnetic island topology are discussed further in Chapter 5.

4.2.7 Event Summary

The combined analysis of the magnetic field, electron velocity, number density, and electron energy distributions provides a consistent picture of a localized magnetic structure within the magnetotail. The bipolar magnetic field signature identifies the presence of a reconnection-related structure, while the accompanying changes in electron velocity and density indicate that the spacecraft encountered a region with plasma properties that differ from the surrounding background. The FPI energy spectra and corresponding energy distribution reveal two distinct electron populations: a dominant bulk population near 10 eV and a broader suprathermal population extending into the keV range. The accompanying FEEPS measurements further demonstrate that a smaller population of electrons is present at energies approaching hundreds of keV, extending the observed energy range beyond that measured by FPI. Taken together, these observations are consistent with the spacecraft crossing a magnetic island-like structure in the magnetotail. Although the magnetic field measurements alone cannot uniquely determine the internal topology of the structure, the combined behavior of the magnetic field and plasma diagnostics provides a consistent interpretation of the event. Comparisons with the remaining events are presented in Chapter 5, where the influence of magnetic topology and plasma environment on the observed electron populations is discussed in greater detail.

4.3 Magnetotail Event 2: July 18, 2017

The second event analyzed in this study occurs in the magnetotail on 18 July 2017 and was selected from previously reported magnetic island observations identified in MMS data by earlier studies (Zhong et al., 2020). In that work, the event was classified as an ion-scale magnetic island observed in the magnetotail and analyzed primarily in terms of magnetic field structure and large-scale plasma flow signatures. In contrast to the original study, which focused on identifying and characterizing the large-scale magnetic topology of the island, the present work re-examines this interval with emphasis on electron-scale dynamics. In particular, the analysis presented here focuses on electron velocity moments and energy distributions in order to investigate how different electron populations behave within the identified magnetic structure.

4.3.1 Magnetic Field Signatures

Figure 4.8 shows the magnetic field components for Event 2. As in Event 1, a clear bipolar signature is observed in the B_z component, indicating a localized magnetic field reversal consistent with a reconnection-related structure.

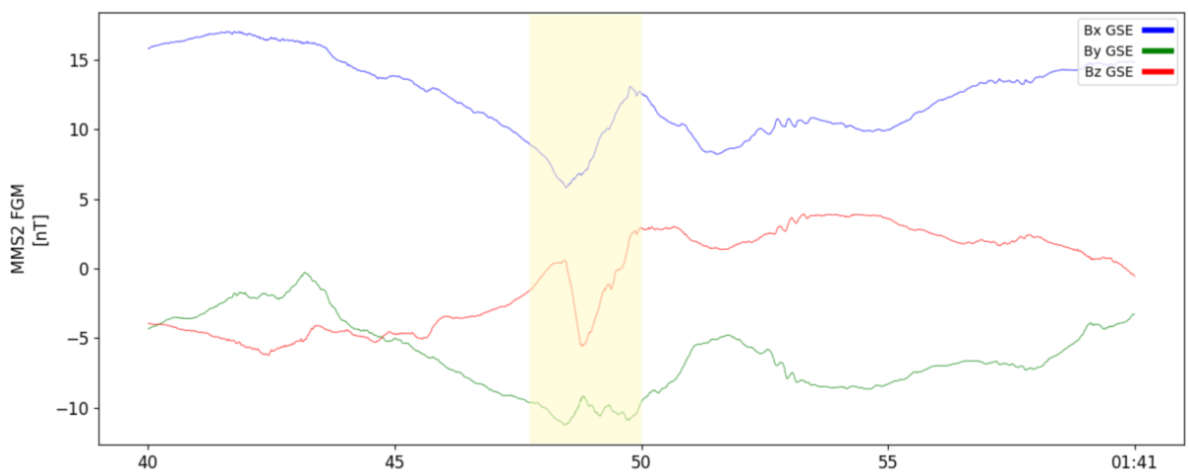

Figure 4. 8 Magnetic field components measured by the MMS FGM instrument in GSE coordinates during the selected magnetotail interval on 18 July 2017. The shaded region highlights the bipolar variation in B_z.

The bipolar signature itself occurs over a short timescale of approximately 1–2 seconds, similar to that observed in Event 1. This suggests that the spacecraft crossing of the central magnetic field reversal region is comparable in duration between the two events. However, the broader magnetic field and plasma environment surrounding this signature extends over a significantly longer interval within the analysis window. This indicates that, while the central reconnection-related crossing is localized in time, the surrounding magnetic structure influencing the electron population is more spatially extended.

4.3.2 Electron Velocity Signatures

The electron velocity components (Figure 4.9) show variations across a broader time interval than the bipolar magnetic signature alone. While the most pronounced changes in velocity are temporally coincident with the bipolar crossing, deviations from background flow conditions persist before and after the bipolar crossing.

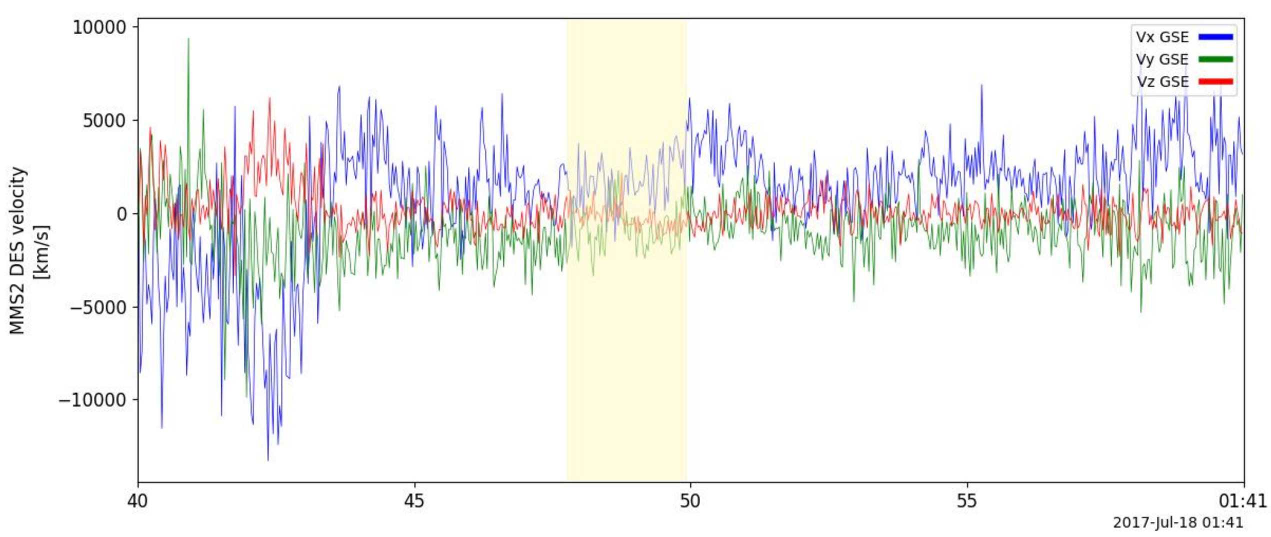

Figure 4. 9 Electron bulk velocity components in GSE coordinates for the selected magnetotail interval. The highlighted region corresponds to the bipolar magnetic signature shown in Figure 4.8.

Compared to Event 1, these velocity variations are gradual in time, suggesting that the spacecraft remains within a region influenced by the magnetic structure for a longer duration. This behavior is consistent with a larger or more extended magnetic island in which electron flows are modified over a wider spatial extent than the central field reversal alone.

4.3.3 Electron Number Density

The electron number density (Figure 4.10) similarly exhibits variations that extend beyond the narrow bipolar magnetic signature. While the most prominent density changes occur near the central crossing region, elevated density levels persist over a larger fraction of the event interval.

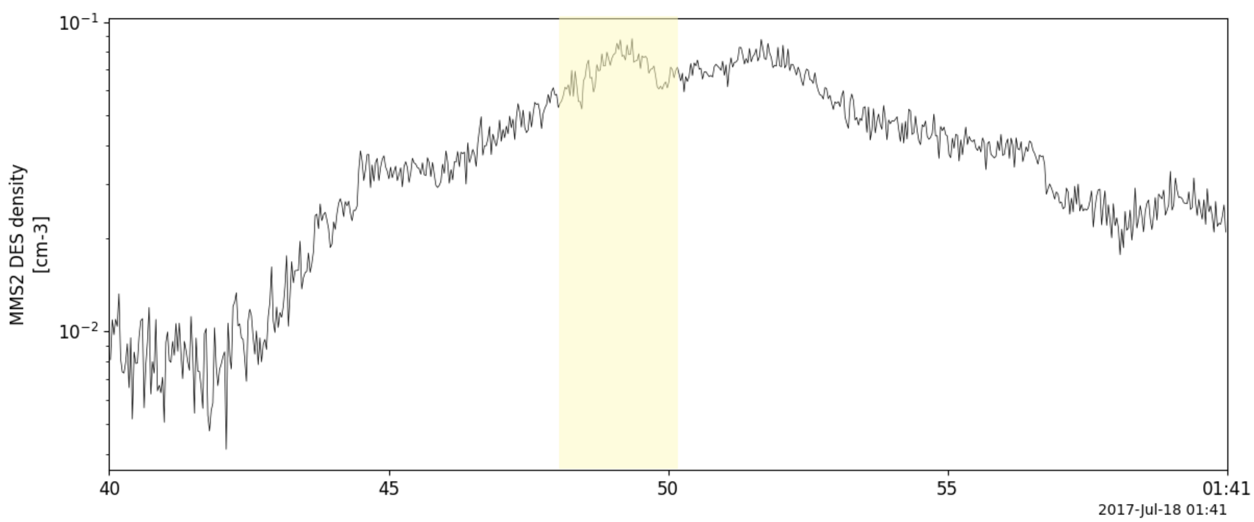

Figure 4. 10 Electron number density during the selected magnetotail interval on 18 July 2017. The highlighted region corresponds to the bipolar magnetic field signature identified in Figure 4.8.

This suggests that plasma confinement or redistribution effects associated with the magnetic island are not limited to the immediate reconnection site but extend across a broader region of the structure. In this sense, the density profile supports the interpretation of a more spatially extended magnetic island when compared to Event 1.

4.3.4 Electron Energy Spectra

Electron energy spectra from the FPI instrument are shown in Figure 4.11 for the selected Event 2 interval. As with Event 1, the bipolar magnetic field signature occurs over a short timescale of approximately 1–2 seconds; however, the electron energy response extends across a substantially larger portion of the 20-second analysis interval. The electron population exhibits sustained changes before and after the magnetic field reversal, indicating that the spacecraft remained within a region influenced by the magnetic structure beyond the immediate bipolar crossing.

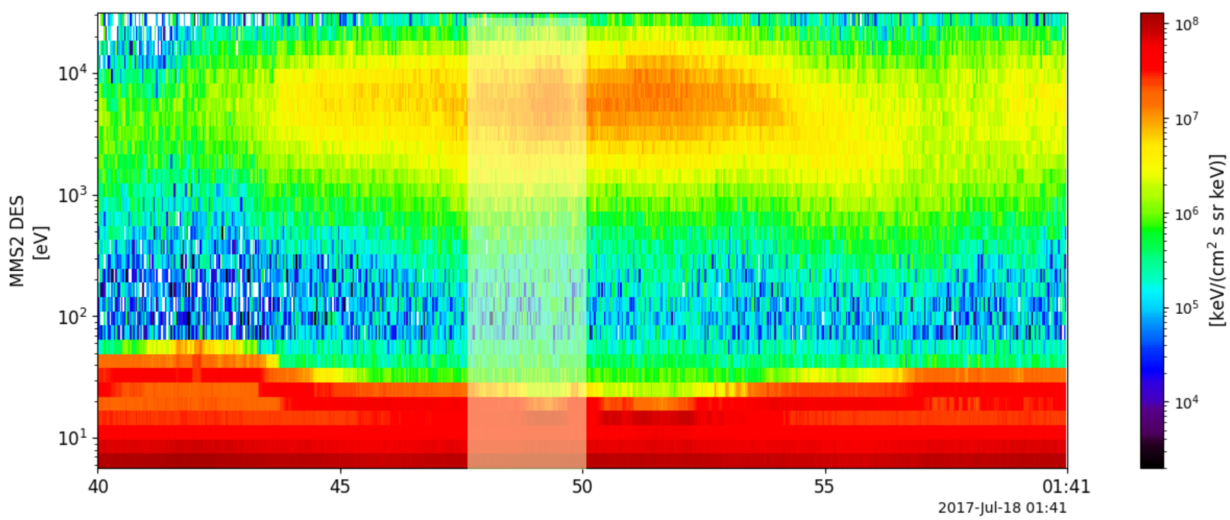

Figure 4. 11 Omni-directional electron energy spectrum measured by the FPI instrument during the selected magnetotail interval on 18 July 2017. The shaded region corresponds to the bipolar magnetic field signature identified in Figure 4.8. The extended electron response surrounding the highlighted interval indicates that changes in the electron population persist beyond the duration of the magnetic field reversal.

Within the FPI energy range (approximately 10^1-10^4 eV), the extended response appears as a prolonged modification of the electron energy distribution. Compared with

Event 1, where the strongest changes were more localized around the identified magnetic structure, Event 2 exhibits changes over a larger fraction of the analyzed interval. This suggests that the spacecraft encountered a broader region of modified electron populations, consistent with a more spatially extended magnetic island-like structure or O-point region.

4.3.5 Electron Energy Distributions

Following the approach used for Event 1, electron energy distributions were calculated using the FPI and FEEPS measurements over the interval associated with the expected O-point region (01:40:45–01:40:54 UTC). This interval was selected based on the combined interpretation of the magnetic field, velocity, density, and energy spectra presented in the previous sections. The distributions provide a comparison of the bulk and energetic electron populations within the magnetic structure. The FPI energy distribution is shown in Figure 4.12(a). Similar to Event 1, the distribution contains two distinct electron populations. A dominant bulk population is observed near approximately 10 eV, representing the background thermal electron population. A second broader population is present between approximately 1 and 10 keV, with a peak near 5–6 keV. Between these two populations, the electron distribution decreases significantly near approximately 100 eV, producing a similar reduction in intermediate-energy electrons observed during Event 1. The suprathermal population in Event 2 extends over a broader energy range compared with the low-energy peak, indicating that electrons within the structure occupy a wide range of energies. The similarity between the energy distributions observed in Events 1 and 2 suggests that both magnetotail structures contain comparable electron population types despite differences in their apparent spatial extent.

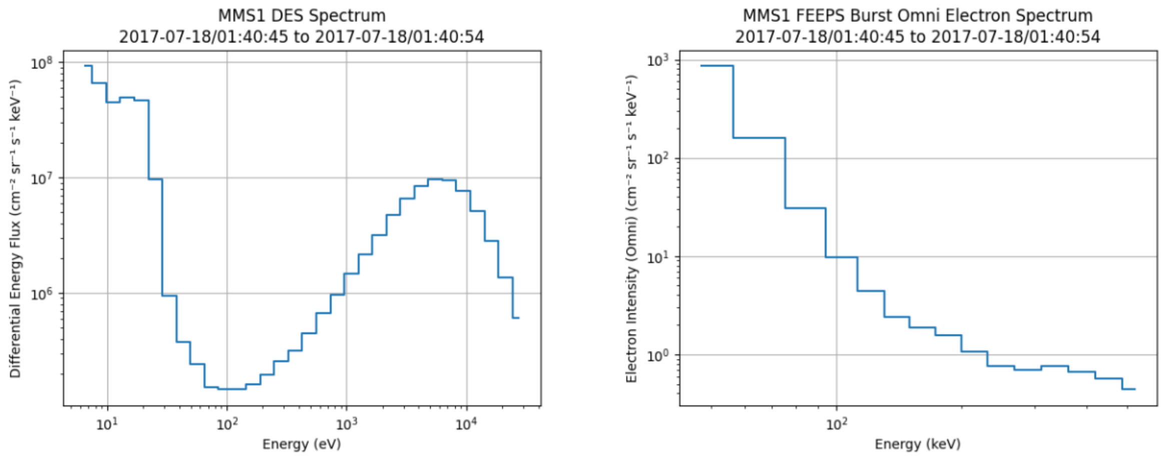

Figure 4. 12 (a) Electron energy distribution derived from FPI measurements for the expected O-point interval of Event 2 (01:40:45–01:40:54 UTC). The distribution shows a dominant bulk electron population near 10 eV and a broader suprathermal population extending from approximately 1 to 10 keV, with a reduced population near 100 eV. (b) Electron energy distribution derived from FEEPS measurements for the expected O-point interval of Event 2. The distribution extends into the tens to hundreds of keV range, demonstrating the presence of a higher-energy electron population beyond the FPI measurement range.

The corresponding FEEPS energy distribution is shown in Figure 4.12(b). This measurement extends the observed electron population into the higher-energy range beyond the FPI measurements. A smaller population of energetic electrons is detected, extending into the tens to hundreds of keV range. Together, the FPI and FEEPS distributions demonstrate that the electron population within Event 2 spans multiple energy regimes, from the bulk population near 10 eV to energetic electrons approaching hundreds of keV. The primary difference compared with Event 1 is not the overall shape of the electron distribution, but rather the larger temporal extent over which these modified electron populations are observed.

4.3.6 Event Summary

Event 2 corresponds to a previously identified magnetotail magnetic island observed in MMS burst-mode measurements (Zhong et al., 2020). The bipolar magnetic field signature occurs over a similar timescale to Event 1 and is consistent with a localized reconnection-related structure. However, the associated electron response extends over a larger fraction of the analyzed interval, indicating that the spacecraft encountered a broader region influenced by the magnetic structure. The FPI and FEEPS energy distributions show electron populations similar to those observed in Event 1, including a dominant bulk population near 10 eV, a broader suprathermal population centered in the keV range, and a smaller energetic electron population extending into higher energies. The persistence of these populations across a larger interval suggests that the interaction region associated with Event 2 extends beyond the narrow magnetic field reversal used to identify the structure.

Overall, Event 2 provides a second example of a magnetotail magnetic island-like structure exhibiting similar electron energy characteristics to Event 1, while also demonstrating a more extended electron response. The comparison between these events and the possible influence of magnetic island size and structure on electron energization are discussed further in Chapter 5.

4.4 Magnetosheath Event: October 25, 2015

The third event analyzed in this study occured in the magnetosheath and corresponds to a previously identified ion-scale magnetic island observed on 25

October 2015 in the interval 11:25:30–11:25:50 in MMS burst-mode data (Huang et al., 2016). In the original study, this interval was examined as part of a broader survey of magnetic islands embedded in turbulent magnetosheath plasma, with emphasis placed on identifying magnetic structures and characterizing ion-scale dynamics. In that work, the analysis primarily focused on the magnetic field topology and ion-scale signatures associated with transient magnetic island formation in a turbulent environment. The event was identified as part of a broader population of magnetosheath islands, rather than as an isolated, long-duration structure. In this study, the interval is revisited with a focus on electron-scale behavior. In particular, the analysis concentrates on how electron velocity moments, density variations, and energy distributions respond within a highly dynamic and turbulent background plasma environment.

4.4.1 Magnetic Field Signatures

Figure 4.13 shows the magnetic field components measured during the selected magnetosheath interval in Geocentric Solar Ecliptic (GSE) coordinates. As in the previous events, the components B_x, B_y, and B_z are used to identify localized magnetic field structures, with particular attention given to rapid reversals in the z-direction.

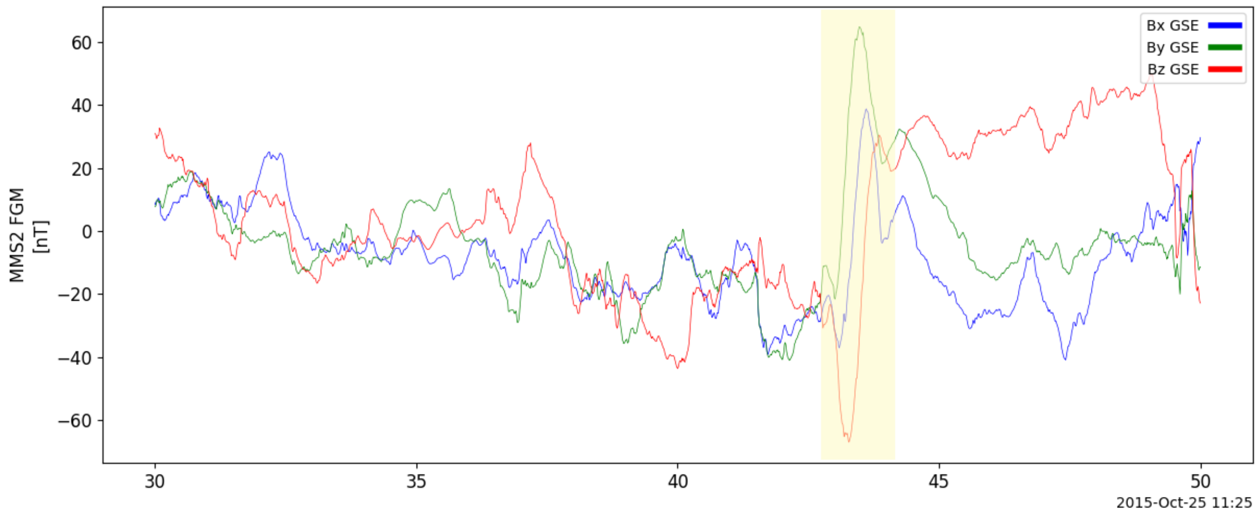

Figure 4. 13 Magnetic field components in GSE coordinates during the interval of 11:25:30 UTC to 11:25:50 UTC on 25 October 2015. The highlighted region indicates the bipolar variation in the out-of-plane magnetic field component. Overall, this interval shows increased magnetic variability compared to the magnetotail events shown in Figures 4.1 and 4.8.

A bipolar signature is clearly observed in the highlighted interval of the B_z component, characterized by a sharp transition from approximately -60 nT to +30 nT over a timescale of roughly 1 second. This represents a significantly stronger magnetic perturbation than that observed in the magnetotail events, where bipolar variations were typically confined to amplitudes on the order of ±5 nT. The increased magnitude is consistent with the generally higher magnetic field strengths present in the magnetosheath environment.

In contrast to the magnetotail cases, this bipolar structure is embedded within a strongly fluctuating magnetic background. Over the full 20-second interval, all magnetic field components exhibit significant variability, indicating a more turbulent plasma environment. While the bipolar feature remains temporally localized, the surrounding magnetic field does not remain quasi-stationary, as was observed in the magnetotail events, making the identification of a single coherent structure more challenging.

Despite this, the most clearly defined bipolar variation remains confined to approximately 1 second within the interval. This temporal localization is used as an indicator for isolating the structure for further plasma analysis in the following sections.

4.4.2 Electron Velocity Signatures

Electron velocity moments measured by the FPI instrument are shown in Figure 4.14. As with the magnetic field measurements, the velocity components exhibit rapid and irregular variations throughout the interval, consistent with a strongly turbulent magnetosheath environment.

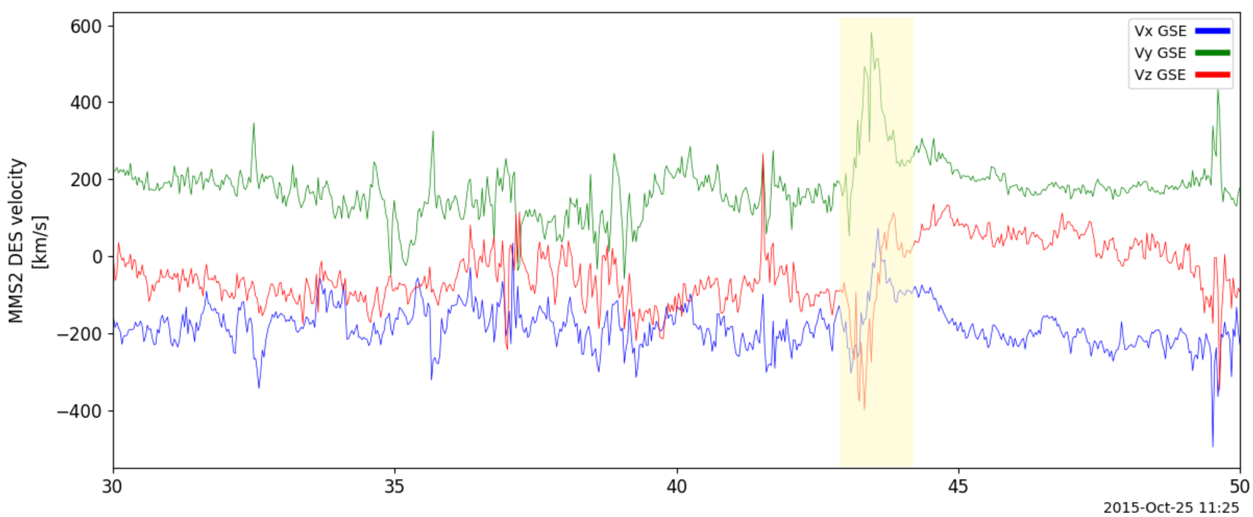

Figure 4. 14 Electron bulk velocity components in GSE coordinates during the selected magnetosheath interval. The shaded region corresponds to the bipolar magnetic field signature shown in Figure 4.13. A brief reversal in flow speed is observed near the center of the interval, coincident with the magnetic structure.

Figure 4.14 shows the electron bulk velocity components in GSE coordinates over the same time interval, with the bipolar magnetic signature region highlighted for comparison. Within the broader turbulent background, the velocity components do not exhibit the same extended periods of coherent flow structure observed in the magnetotail events. However, within the highlighted interval, the electron bulk velocity undergoes a localized reversal that coincides with the bipolar magnetic field signature shown in Figure 4.13. Both V_x and V_z change direction across the highlighted interval, indicating a localized flow reversal rather than an extended stagnation region. Unlike the magnetotail events, where coherent flow structures persist over longer time intervals, this reversal is confined to a narrow region embedded within the surrounding turbulent plasma. Such localized velocity reversals are consistent with a spacecraft crossing near a reconnection X-point or another rapidly evolving magnetic topology, although the available observations do not uniquely determine the underlying structure.

4.4.3 Electron Number Density

The electron number density measured during the event is shown in Figure 4.15. As with the magnetic field and velocity measurements, the density exhibits strong variability throughout the interval, with fluctuations occurring on timescales comparable to or shorter than the duration of the bipolar magnetic signature.

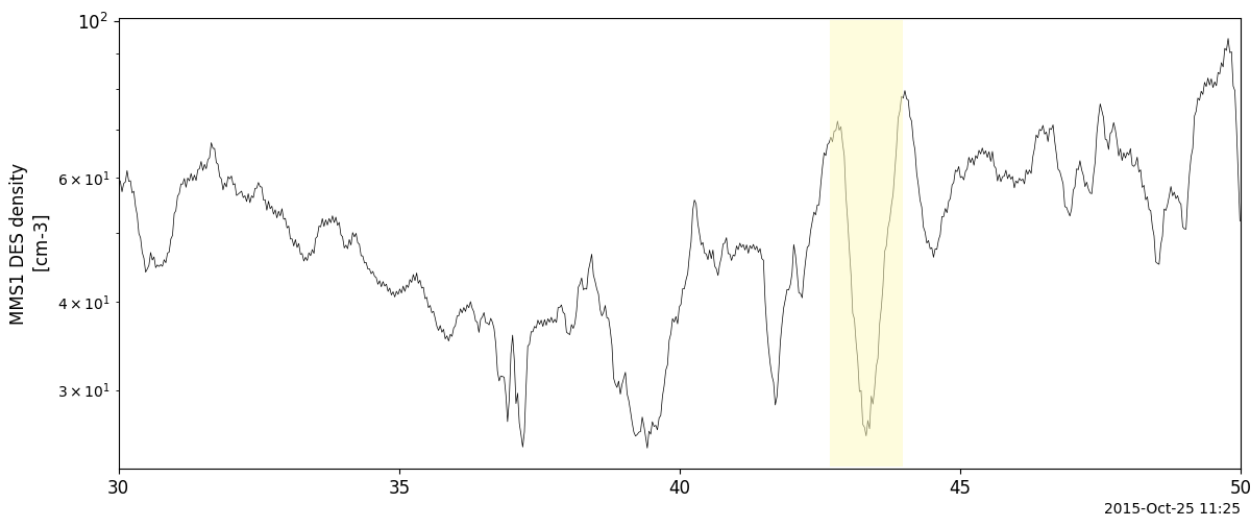

Figure 4. 15 Electron number density during the selected magnetosheath interval. The shaded region indicates the bipolar magnetic field signature shown in Figure 4.13. Density peaks are observed on either side of the structure, with a localized depletion near the center of the interval.

Figure 4.15 shows the electron number density over the same interval, with the bipolar magnetic field region highlighted for comparison. In contrast to the magnetotail events, there is no sustained period of increased or depleted density. Instead, the density profile exhibits two localized maxima on either side of the bipolar crossing, with a pronounced decrease near the center of the interval. This structure is notably different from the magnetotail cases, where density enhancements were more consistently aligned with the central region of the magnetic structure and were interpreted as possible signatures of particle trapping near island cores. In this event, the density minimum at the center of the bipolar signature, together with the flanking density peaks, is more consistent with a crossing between regions of compressed plasma rather than a single coherent island core. This suggests that the bipolar magnetic signature in this case may correspond to a different part of the reconnection geometry, such as a separatrix region or X-line crossing, rather than an O-point crossing as was more consistent with the magnetotail events. However, given the highly turbulent nature of the magnetosheath environment, this interpretation is not unique and is further examined using the energy spectrum in the following section.

4.4.4 Electron Energy Spectra

The electron energy spectra measured by the FPI instrument for the full 20-second interval are shown in Figure 4.16. This extended view is used to maintain consistency with the presentation of the previous events and to provide context for the overall plasma environment in which the magnetic structure occurs. In this representation, the spectrogram shows broadband variability in electron intensity across the interval, although the short-duration features associated with the bipolar magnetic signature are not immediately distinguishable at this temporal scale.

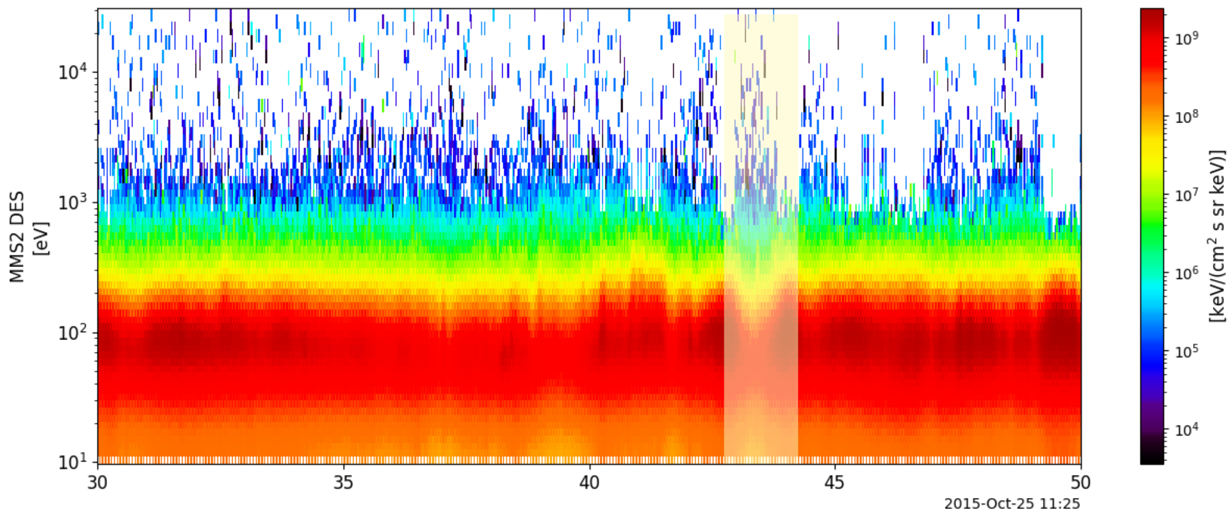

Figure 4. 16 Omni-directional electron energy spectrum during the full 20-second magnetosheath interval. The shaded region indicates the bipolar magnetic field signature shown in Figure 4.13. At this temporal scale, short-duration electron energization features are not readily resolved.

To better resolve the localized structures identified in the magnetic field and plasma moment analysis, a zoomed-in view of the energy spectra is shown in Figure 4.17, covering a reduced interval of approximately 6 seconds centered on the bipolar magnetic signature. In this higher-resolution view, two distinct enhancements in electron intensity can be identified on either side of the central crossing, with a localized feature occurring at the time of the bipolar magnetic field reversal.

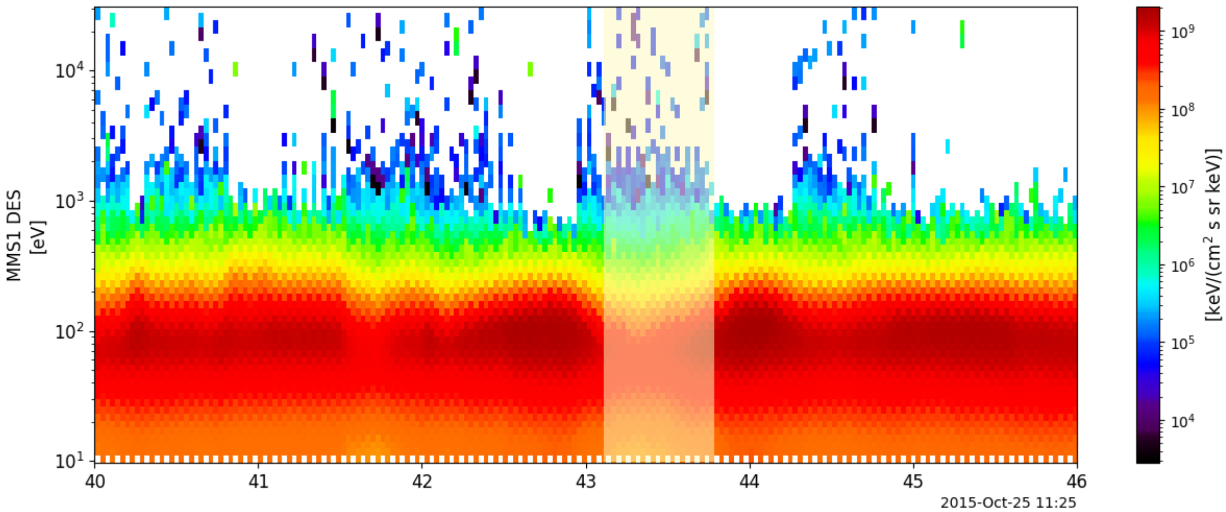

Figure 4. 17 Zoomed in omni-directional electron energy spectrum for a reduced interval roughly centered on the bipolar magnetic field signature (highlighted). Two localized enhancements in electron intensity are observed on either side of the central crossing, with a transition region corresponding to the magnetic field reversal.

Within this zoomed interval, the electron population exhibits a pronounced energy increase, in the keV range, between the two density peaks. The central region of the bipolar signature aligns with a transition between these populations. This structure is consistent with the interpretation that the spacecraft crosses a boundary region separating two adjacent magnetic structures, rather than remaining within a single coherent island throughout the interval. In this context, the bipolar magnetic signature is more consistent with either an X-point crossing or a separatrix region between adjacent magnetic islands, where changes in magnetic field lines lead to localized enhancements in energetic electron flux. This interpretation is supported by the combined observation of density depletion at the center (Figure 4.15), velocity reduction (Figure 4.14), and adjoining density enhancements, all of which suggest that the spacecraft traverses a boundary region. However, given the turbulent nature of the region, this interpretation is not unique and is further discussed in Chapter 5.

4.4.5 Electron Energy Distribution

To further characterize the electron population associated with the magnetosheath structure, an energy histogram was constructed using FPI measurements over the interval corresponding to the left-side magnetic island region identified in the energy spectrum analysis. Unlike the magnetotail events, the electron energy distribution in Event 3 occurs primarily within the lower-energy range measured by FPI, and the higher-energy FEEPS measurements were not required for interpretation of this event. The selected interval is limited to the nearest available one-second resolution, which results in a small amount of overlap between the selected region and adjacent portions of the structure. Therefore, the resulting distribution represents the electron population associated with the island region and its immediate surroundings rather than an isolated measurement of the island center alone.

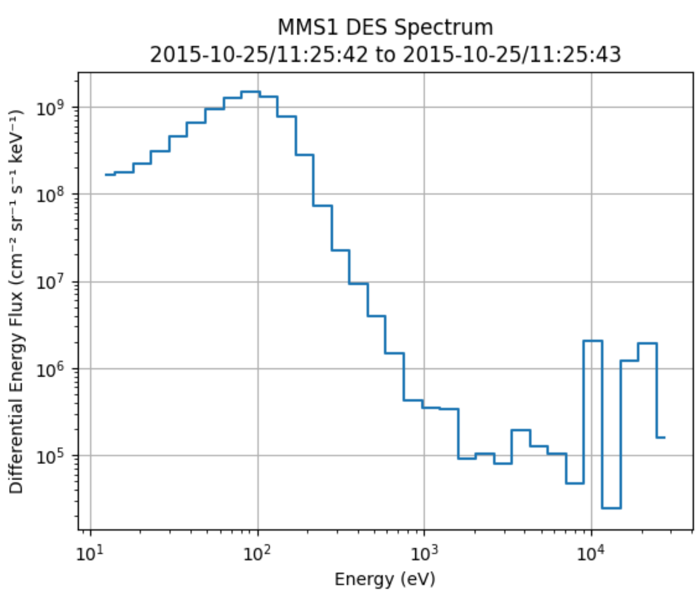

Figure 4. 18 Electron energy histogram derived from FPI measurements for the left-side magnetic island region in Event 3. The distribution is dominated by a low-energy electron population near approximately 100 eV, with a smaller suprathermal population extending toward the keV range.

The resulting energy distribution differs significantly from the magnetotail events. Instead of the two distinct populations observed in Events 1 and 2, consisting of a thermal population near approximately 10 eV and a suprathermal population extending into the keV range, Event 3 exhibits a dominant electron population centered near approximately 100 eV. This energy range corresponds to the region where a depletion was observed in the magnetotail events, suggesting that the characteristic electron energies within the magnetic structure are strongly influenced by the surrounding plasma environment. In addition to the dominant low-energy population, a smaller enhancement is observed at higher energies extending into the ~10 keV range. However, this energetic population should be interpreted cautiously, as the selected one-second interval includes portions of the surrounding structure where enhanced energetic electron signatures are observed in the energy spectra. These higher-energy electrons are therefore consistent with the localized energetic enhancements identified near the boundaries of the magnetic structure, but the histogram alone cannot determine the exact spatial origin of these electrons.

Unlike the magnetotail events, Event 3 exhibited only weak energetic electron signatures in the FEEPS energy range, so the primary analysis focused on the FPI measurements. In Events 1 and 2, energetic electrons extending into tens to hundreds of keV required measurements from FEEPS to characterize the higher-energy population. In contrast, the dominant electron response in Event 3 occurs within the FPI energy range, with the primary features of interest occurring below approximately 10 keV. Overall, the electron energy distribution in Event 3 demonstrates that magnetic island-associated electron populations can occur across substantially different energy regimes. While the magnetotail events are characterized by separated thermal and suprathermal populations, the magnetosheath event is dominated by a lower-energy electron population with short-lived enhancements at higher energies.

4.4.6 Event Summary

Event 3 corresponds to a previously identified magnetosheath magnetic island observed on 25 October 2015 (11:25:40–11:25:46 UTC) (Huang et al., 2016). The original study investigated this interval as part of a broader analysis of ion-scale magnetic islands in the turbulent magnetosheath, with emphasis on magnetic field structure and plasma characteristics. The present analysis focuses on the electron-scale response associated with this structure. Compared with the magnetotail events, Event 3 exhibits a shorter-lived and more dynamic response, with stronger fluctuations in the surrounding magnetic field, velocity, and density measurements. The electron energy distribution is also shifted toward lower energies, with the dominant population occurring near approximately 100 eV rather than the 10 eV and keV-scale populations observed in Events 1 and 2.

Although the bipolar magnetic signature is localized in time, energetic electron enhancements are observed near the surrounding magnetic structures rather than directly centered on the magnetic reversal. These observations are consistent with electron energization occurring near localized reconnection regions within a highly dynamic plasma environment, where multiple short-lived structures may form and evolve over rapid timescales. Further interpretation of the differences between magnetotail and magnetosheath electron responses is discussed in Chapter 5.

Chapter 5 Discussion

5.1 Comparison of Magnetotail and Magnetosheath Events

Although all three events examined in this study exhibit localized bipolar magnetic field measurements consistent with reconnection-related structures, the associated electron behavior differs considerably between the magnetotail and magnetosheath environments. These differences are observed not only in the characteristic electron energies, but also in the temporal extent of the structures, the distribution of energetic electrons, and the relationship between magnetic field signatures and plasma moments. The two magnetotail events display relatively similar behavior despite occurring during different intervals. In both cases, the bipolar magnetic field signature is confined to a short interval of approximately one to two seconds, while the associated electron response extends over a much longer period of time. Variations in electron velocity, density, and energy distributions persist both before and after the magnetic field reversal, suggesting that the spacecraft is sampling a larger magnetic structure surrounding the localized reversal region. This extended electron response is consistent with an O-point crossing, where trapped plasma populations can occupy a broader region than the central magnetic signature alone would indicate. In contrast, the magnetosheath event exhibits a different relationship between the magnetic field signature and electron response. The localized velocity reversal, density depletion, and surrounding density enhancements near the bipolar magnetic signature suggest a structure more consistent with an X-point or separatrix crossing rather than an extended O-point region. However, the turbulent magnetosheath environment and limited duration of the event make this interpretation less certain, and additional measurements would be required to confirm the underlying magnetic topology.

The characteristic electron energies in the magnetotail events are also considerably higher than those observed in the magnetosheath event. The dominant suprathermal electron populations in Events 1 and 2 occur primarily in the 10^3-10^4 eV range, with energetic electrons extending into the FEEPS energy range of tens to hundreds of keV. In contrast, the background plasma in the magnetosheath event is centered near approximately 10^2 eV, while the highest energy electron populations occur closer to the 10^3 eV range. One possible explanation for this difference is the substantially different plasma environments in which the structures form. The magnetotail current sheet is generally characterized by lower magnetic fluctuations and longer-lived reconnection structures, allowing magnetic islands to persist for longer periods of time and potentially grow to larger spatial scales (Eastwood et al., 2015; Burch et al., 2016). In contrast, the magnetosheath is highly dynamic and turbulent due to the interaction between the solar wind and the terrestrial bow shock (Yordanova et al., 2016; Phan et al., 2018). Magnetic structures embedded within this environment may evolve more rapidly and therefore provide less time for particle trapping and energization processes to occur.

The results of this study suggest that island size and lifetime may play an important role in determining the resulting electron energy distributions. Event 2 provides a particularly interesting example of this behavior. Although the bipolar magnetic signature itself remains localized to approximately one to two seconds, the electron response extends across nearly the entire twenty-second analysis interval.

Compared to Event 1, the energetic electron populations in Event 2 remain elevated over a broader temporal region and the distinction between island core and boundary populations becomes less pronounced. If the temporal extent of the electron response reflects the spatial size of the underlying magnetic structure, these observations may indicate that larger islands are capable of influencing electrons over greater distances and longer timescales. Such structures may allow particles to remain trapped for longer periods, increasing the likelihood of repeated acceleration through reconnection electric fields or multiple interactions with contracting magnetic field lines. While this work cannot directly determine island size from single-spacecraft observations, the observations are consistent with previous theoretical and simulation studies suggesting that larger magnetic islands can support more efficient particle energization (Drake et al., 2006; Oka et al., 2010; Guo et al., 2014).

The magnetosheath event exhibits a different behavior. Rather than observing broad enhancements extending throughout the structure, energetic electrons appear as more localized and sharply defined populations. In addition, the density profile and energy spectra suggest that the bipolar magnetic signature may correspond to a boundary region between adjacent magnetic structures rather than the center of a single island. This interpretation is supported by the presence of density enhancements on either side of the bipolar crossing together with enhanced energetic electron populations located between these features. An important result of this study is therefore that bipolar magnetic signatures alone are insufficient to uniquely identify magnetic topology. Depending on the spacecraft trajectory and local plasma conditions, a bipolar crossing may correspond to an O-point, an X-point, a separatrix crossing, or another reconnection-related boundary (Eastwood et al., 2010; Burch et al., 2016; Zhou et al., 2019). Additional diagnostics, including plasma moments, density structure, and energetic particle measurements, are necessary to distinguish between these possibilities.

Despite the differences between the events, a common feature is that electron populations are not distributed uniformly throughout the structures. Instead, both the FPI and FEEPS measurements indicate that electron energies vary systematically across different regions of the magnetic topology. This observation is consistent with the broader picture emerging from both simulations and spacecraft observations in which magnetic topology plays a fundamental role in controlling particle trapping, transport, and acceleration.

5.2 Implications for Laboratory and Space Plasmas

One of the primary motivations for this work is the possibility that common physical processes govern energetic electron transport in both laboratory and space plasmas despite the enormous differences in their physical scales. Tokamak plasmas and Earth's magnetosphere differ by many orders of magnitude in size, magnetic field strength, density, and characteristic timescales. However, both systems develop magnetic islands through changes in magnetic topology, providing an opportunity to investigate whether similar electron dynamics occur in both environments.

The DIII-D experiments associated with this broader research project examined the interaction between energetic electrons and magnetic islands formed within a controlled laboratory plasma. Rather than relying on single-point spacecraft measurements, the laboratory experiments were able to observe the spatial evolution of energetic electrons across the island using various emission diagnostics, including synchrotron emission, electron cyclotron emission, and hard X-rays. These measurements demonstrated that changes in magnetic island topology strongly influence energetic electron transport, with electron confinement and loss depending on the structure and dynamics of the island itself. One particularly important result from the DIII-D experiments is that magnetic islands can both confine energetic electrons and provide pathways for their rapid transport when the island structure changes (Eskew et al., 2026) During periodic island bifurcation on the q=2 magnetic surface, bursts of energetic electrons were observed escaping confinement. These observations indicate that electron transport is governed not only by the presence of a magnetic island alone, but also by its geometry, width, and temporal evolution.

Although the present study does not directly measure island dynamics, the MMS observations show several qualitative similarities. In the two magnetotail events, the electron response extends well beyond the narrow bipolar magnetic field signature used to identify the magnetic structure. Electron density, bulk velocity, and energy spectra all remain modified over a broader interval than the magnetic field reversal itself. This suggests that the surrounding magnetic topology influences electron motion over a region larger than the localized current sheet crossing detected by the spacecraft. The magnetosheath event provides a somewhat different perspective. Rather than observing a relatively isolated magnetic structure embedded within a quiet plasma sheet, the spacecraft encountered a highly dynamic magnetic environment containing rapid magnetic field fluctuations and multiple localized electron energization sites. The analysis suggests that the bipolar magnetic signature most likely corresponds to a reconnection region or boundary separating neighboring magnetic islands rather than the center of a single coherent island. Energetic electron enhancements occur adjacent to this region, consistent with particle acceleration occurring near reconnection sites identified in previous MMS studies (Huang et al., 2016; Hasegawa et al., 2022). Taken together, the laboratory and spacecraft observations support the idea that magnetic topology plays an important role in energetic electron transport across a wide range of plasma conditions. In both systems, electrons do not simply respond to the local magnetic field strength but instead to the larger magnetic topology created by reconnection and island formation. While the spatial and temporal scales differ dramatically, the observations suggest that magnetic islands affect electron motion through similar physical mechanisms.

At the same time, important differences remain between the laboratory and space environments. The DIII-D experiments provide controlled plasma conditions in which island size, location, and evolution can be deliberately modified, allowing repeated measurements of electron transport under nearly identical conditions. In contrast, spacecraft measurements provide only a one-dimensional trajectory through naturally evolving structures whose full geometry cannot be directly reconstructed from a single spacecraft. Consequently, the comparisons between the two systems are necessarily qualitative. Nevertheless, the agreement in the overall behavior of energetic electrons provides encouraging evidence that laboratory experiments can complement spacecraft observations when investigating fundamental reconnection physics.

These similarities support one of the central hypotheses motivating this work: that magnetic island topology represents a scalable physical process influencing energetic electron transport across laboratory and space plasmas. Although additional observations and more detailed multi-spacecraft analyses are required before quantitative scaling relationships can be established, the present results demonstrate that the interaction between energetic electrons and magnetic islands exhibits consistent qualitative behavior in both environments.

5.3 Limitations and Future Work

Several limitations of the present study should be considered when interpreting these results. First, the analysis relies primarily on measurements from a single MMS spacecraft during each event interval. While single-spacecraft measurements are sufficient to identify localized magnetic signatures and associated plasma behavior, they do not allow direct reconstruction of the three-dimensional magnetic topology or determination of the true spatial extent of the structures. Multi-spacecraft timing analysis using all four MMS spacecraft would provide additional information regarding island motion, propagation speed, and physical size.

Second, the analysis was performed entirely in Geocentric Solar Ecliptic coordinates rather than in a local LMN coordinate system derived from minimum variance analysis or multi-spacecraft techniques. Although GSE coordinates were sufficient for identifying the major features considered in this work, transformation into LMN coordinates would allow a more physically meaningful separation of inflow, outflow, and guide field directions and would simplify comparisons with reconnection simulations and previous studies.

A further limitation is the relatively small number of events considered in the present analysis. The conclusions presented here are based on two magnetotail events and a single magnetosheath event and therefore should not be interpreted as universal properties of magnetic islands in these environments. A larger statistical survey involving many more events would be required to determine whether the trends observed here are representative of magnetotail and magnetosheath reconnection more generally.

Finally, although the original motivation for this work involved comparisons between magnetic islands in laboratory and space plasmas, only qualitative comparisons were performed in the present study. Future work could investigate whether common scaling relationships exist between island size, magnetic field strength, and energetic electron populations in both environments. Such studies would help determine whether magnetic islands in laboratory and space plasmas belong to the same universality class despite their vastly different physical scales. Overall, the results presented here suggest that magnetic topology plays an important role in shaping electron behavior in reconnection environments and that similar physical mechanisms may operate across a wide range of plasma systems.

References

Angelopoulos, V., et al. (2008). Tail reconnection triggering substorm onset. *Science*, 321(5891), 931–935. DOI: 10.1126/science.1160495

Burch, J. L., et al. (2016). Magnetospheric Multiscale Overview and Science Objectives. *Space Science Reviews*, 199, 5–21. DOI: 10.1007/s11214-015-0164-9

Chen, L. J., Bessho, N., Lefebvre, B., et al. (2011). Multispacecraft observations of electron acceleration in magnetic islands and associated magnetic reconnection. *Physics of Plasmas, 18*, 012901.

Chen, L.J., et al. (2008). Observation of energetic electrons within magnetic islands. *Nature Physics*, 4, 19–23. DOI: 10.1038/nphys777

Drake, J. F., Swisdak, M., Che, H., & Shay, M. A. (2006). Electron acceleration from contracting magnetic islands during reconnection. *Nature*, 443, 553–556. DOI: 10.1038/nature05116

Eastwood, J. P., et al. (2010). The science of space weather. *Philosophical Transactions of the Royal Society A*, 368, 4489–4500. DOI: 10.1098/rsta.2010.0171

Escoubet, C. P., Fehringer, M., & Goldstein, M. (2001). The Cluster mission. *Annales Geophysicae*, 19, 1197–1200. DOI: 10.5194/angeo-19-1197-2001

Eskew, J., Orlov, D.M., et al. (2026). Effect of controlled magnetic island bifurcation on electron diffusion. *Nucl. Fusion* 66 066022. DOI: 10.1088/1741-4326/ae6ab3

Eskew, J., Battles, S., Ostermeier, S.J., Cote, T.B., Koepke, M.E., Skiff, F.N., Austin, M.E., Marini, C., Orlov, D.M., and Kostadinova, E.G. DIII-D Frontiers Experiments Reveal the Interaction of Energetic Electrons and Magnetic Islands Confirming Major Findings of the MMS Mission. *In 67th Annual Meeting of the APS Division of Plasma Physics*. 2025.

Grimes E.W., et al. (2022) The Space Physics Environment Data Analysis System in Python. Front. Astron. Space Sci. 9:1020815. DOI: 10.3389/fspas.2022.1020815

Hasegawa, H., et al. (2022). Magnetic Field Annihilation in a Magnetotail Electron Diffusion Region With Electron-Scale Magnetic Island. *Journal of Geophysical Research: Space Physics*, 127. DOI: 10.1029/2022JA030408

Horton, C.W., Ichikawa, Y.H., *Chaos and Structures in Nonlinear Plasmas*. World Scientific, 1996.

Huang, S. Y., et al. (2016). MMS observations of ion-scale magnetic island in the magnetosheath turbulent plasma. *Geophysical Research Letters*, 43, 7850–7858. DOI: 10.1002/2016GL070033

Huang, S. Y., et al. (2019). Observations of Flux Ropes With Strong Energy Dissipation in the Magnetotail. *Geophysical Research Letters*, 46. DOI: 10.1029/2018GL081099

Imperial College London, "Fluxgate Magnetometers," Space Magnetometer Laboratory, https://www.imperial.ac.uk/space-and-atmospheric-physics/research/areas/space-magnetometer-laboratory/space-instrumentation-research/magnetometers/fluxgate-magnetometers/ (accessed July 20, 2026).

Joseph, I. et al., “Calculation of stochastic thermal transport due to resonant magnetic perturbations in DIII-D,” *Nucl. Fusion*, vol. 48, no. 4, p. 045009, Mar. 2008, doi: 10.1088/0029-5515/48/4/045009.

Kavosi, S., Raeder, J., Johnson, J.R. et al. Seasonal and diurnal variations of Kelvin-Helmholtz Instability at terrestrial magnetopause. *Nat Commun* **14**, 2513 (2023). https://doi.org/10.1038/s41467-023-37485-x

Kostadinova, E.G., Orlov, D.M., Koepke M., Skiff, F., Austin, M.E. Energetic electron transport in magnetic fields with island chains and stochastic regions. *Journal of Plasma Physics*. 2023;89(4):905890420. doi:10.1017/S0022377823000879

Mauk, B. H., Blake, J. B., Baker, D. N., et al. (2016). The Energetic Particle Detector (EPD) Investigation and the Energetic Ion Spectrometer (EIS) for the Magnetospheric Multiscale (MMS) Mission. *Space Science Reviews, 199*(1–4), 471–514. DOI: 10.1007/s11214-014-0055-5

MMS Science Data Center, *Magnetospheric Multiscale (MMS) Science Data Center*, https://lasp.colorado.edu/mms/sdc/public/ (accessed July 20, 2026)

Nishida, A. (1994). The GEOTAIL mission. *Geophysical Research Letters*, 21(25), 2871–2873. DOI: 10.1029/94GL01223

Norgren, C., Hesse, M., Graham, D. B., Khotyaintsev, Y. V., Tenfjord, P., Vaivads, A., et al. (2020). Electron acceleration and thermalization at magnetotail separatrices. Journal of Geophysical Research: Space Physics, 125, e2019JA027440. https://doi.org/10.1029/2019JA027440

Paschmann, G., et al. (1979). Plasma acceleration at the Earth's magnetopause: Evidence for reconnection. *Nature*, 282, 243–246. DOI: 10.1038/282243a0

Paschmann, G., Haaland, S. E., & Treumann, R. A. (Eds.). (1998). *Analysis Methods for Multi-Spacecraft Data*. ISSI Scientific Report SR-001. Bern, Switzerland: International Space Science Institute.

Pollock, C., et al. (2016). Fast Plasma Investigation for Magnetospheric Multiscale. *Space Science Reviews*, 199, 331–406. DOI: 10.1007/s11214-016-0245-4

Russell, C. T., et al. (2016). The Magnetospheric Multiscale Magnetometers. *Space Science Reviews*, 199, 189–256. DOI: 10.1007/s11214-014-0057-3

Smith, A. W., et al. (2024). Ion-Scale Magnetic Flux Ropes and Loops in Earth's Magnetotail: An Automated, Comprehensive Survey of MMS Data Between 2017 and 2022. *Journal of Geophysical Research: Space Physics*. DOI: 10.1029/2023JA032231

Torbert, R. B., et al. (2018). Electron-scale dynamics of the diffusion region during symmetric magnetic reconnection in space. *Science*, 362(6421), 1391–1395. DOI: 10.1126/science.aat2998

W. W. Heidbrink, W.W., White, R.B. “Mechanisms of energetic-particle transport in magnetically confined plasmas,” *Phys. Plasmas*, vol. 27, no. 3, p. 030901, Mar. 2020, doi: 10.1063/1.5136237.

Wu, M., Lu, Q., Volwerk, M., et al. (2013). Magnetic reconnection associated with electron acceleration in the magnetotail. *Journal of Geophysical Research: Space Physics, 118*, 2112–2122.

Yamada, M., Kulsrud, R., & Ji, H. (2010). Magnetic reconnection. *Reviews of Modern Physics*, 82, 603–664. DOI: 10.1103/RevModPhys.82.603

Zhong, Z. H., Zhou, M., Tang, R. X., Deng, X. H., Turner, D. L., Cohen, I. J., et al. (2020). Direct evidence for electron acceleration within ion-scale flux rope. Geophysical Research Letters, 47, e2019GL085141. https://doi.org/10.1029/2019GL085141